DIELECTRIC PROPERTIES OF COLLOIDAL SUSPENSIONS

Lei Dong

Department of Applied Physics
Helsinki University of Technology
Espoo, Finland

Dissertation for the degree of Doctor of Science in Technology to be presented with due permission of the Faculty of Information and Natural Sciences for public examination and debate in Auditorium E at Helsinki University of Technology (Espoo, Finland) on the 19th of January, 2009, at 13 o'clock.

Dissertations of Department of Applied Physics
Helsinki University of Technology
ISSN 1797-9595 (print)
ISSN 1797-9609 (online)

Dissertation 155 (2009):
Lei Dong: Dielectric properties of colloidal suspensions

Opponent:
Prof. Kai Nordlund, Helsinki University, Finland

Pre-examiners:
Dr. André H Juffer, University of Oulu, Finland
Prof. Apichart Linhannta, Lakehead University, Canada

ISBN 978-951-22-9715-3 (print)
ISBN 978-951-22-9716-0 (electronic)

Picaset Oy
Helsinki 2009

ABSTRACT OF DOCTORAL DISSERTATION	HELSINKI UNIVERSITY OF TECHNOLOGY P. O. BOX 1000, FI-02015 TKK http://www.tkk.fi

Author Lei Dong

Name of the dissertation

Dielectric properties of colloidal suspensions

Manuscript submitted 14.10.2008	Manuscript revised 12.12.2008
Date of the defence 19.01.2009 at 13 o'clock, TKK main building, Otakaari 1, lecture hall E	
☐ Monograph	☒ Article dissertation (summary + original articles)

Faculty	Faulty of Information and Natural Sciences
Department	Department of Applied Physics
Field of research	Soft condensed matter physics
Opponent(s)	Prof. Kai Nordlund, Helsinki University
Supervisor	Acad. Prof. Risto Nieminen
Instructor	Prof. Mikko Karttunen

Abstract

This thesis focuses on theoretical research of dielectric properties of colloidal suspensions in which the suspended particles can be either homogeneous or graded. Colloids have enormous advantages of being experimentally accessible. Atomic size scale, time scale of diffusion and tunable interactions of colloids make them as ideal tools for fundamental investigations. Effective dielectric constant plays a key role in the investigation of the properties of colloidal suspension. Many applications such as dielectrophoresis (DEP) and electrorotation are useful to study the effective dielectric constant.

In the first part of this thesis, a theoretical study of the dielectrophoretic spectrum of a pair of touching colloidal particles is present. The multiple image method is employed to account for the effective dipole factor, and an analytical expression for the DEP force is obtained. It is found that, at low frequency, the DEP force can be enhanced (reduced) significantly for the longitudinal (transverse) field case due to the presence of multiple images.

The second part of the thesis investigates the dielectric properties of functionally graded materials using different methods. Analytical approaches such as Bergman-Milton spectral representation theory and first-principles approach have been generalized to study the dielectric properties of graded composite. Differential effective multipole moment approximation has been developed to study the multipole polarizability of a graded spherical particle in a nonuniform electric field. An anisotropic differential effective dipole approximation has been developed for calculating the dipole moment of anisotropic graded materials. We compared the approximative results with the analytical results and the agreement is excellent. Furthermore, the optical nonlinear response of graded films was studied in this thesis, and the result shows that the composition-dependent gradation can produce a broad resonant plasmon band in the optical region, resulting in a large enhancement of the optical nonlinearity.

Keywords Dielectric properties, Functionally graded materials, Colloid, Suspension	
ISBN (printed) 978-951-22-9715-3	ISSN (printed) 1797-9595
ISBN (pdf) 978-951-22-9716-0	ISSN (pdf) 1797-9609
Language English	Number of pages 67p. + app. 38p.
Publisher Department of Applied Physics, Helsinki University of Technology	
Print distribution Department of Applied Physics, Helsinki University of Technology	
☒ The dissertation can be read at http://lib.tkk.fi/Diss/2009/isbn9789512297160/	

Preface

The work reported in this thesis was carried out at the Helsinki University of Technology (TKK) Biological and Soft Matter Physics group led by Prof. Mikko Karttunen. I would like to express my sincere gratitude to him. Without his advise and unique support this thesis would never become a reality. Further I would like to thank my co-supervisor Prof. Kin Wah Yu at The Chinese University of Hong Kong for his inspiring and active guidance. I would also like to thank Prof. Risto Nieminen who leads COMP group in Laboratory of Physics and Prof. Kimmo Kaski who leads Laboratory of Computational Engineering for providing excellent facilities and working environment.

I would like to express my gratitude to all the co-authors of the publications related to this thesis. I wish to thank Prof. Ji-Ping Huang at Fudan University, who raised the questions and taught me how to answer them; special thanks belong to Prof. Guo-Qing Gu at East China Normal University, who led me to the beautiful mathematical world; and many thanks for Dr. En-Bo Wei for discussions and collaborations.

Beside colleagues, I have been lucky to have plenty of peer support in my study. Many thanks are devoted to my dear friends for letting me share the good and bad moments, and for your kind help with my study and life in Finland.

I owe much to my parents who have never shown anything but support and belief in me. Finally, I would like to thank my husband Shunyong for his support, patience, and love all through these years.

Otaniemi, November 2008

Lei Dong

Contents

List of publications

This dissertation consists of an overview and the following publications:

I. L. Dong, J. P. Huang, and K. W. Yu, *Theory of dielectrophoresis in colloidal suspensions*, J. Appl. Phys. **95**, 8321 (2004).

II. L. Dong, J. P. Huang, K. W. Yu, and G. Q. Gu, *Dielectric response of graded spherical particles of anisotropic materials*, J. Appl. Phys. **95**, 621 (2004).

III. J. P. Huang, L. Dong, and K. W. Yu, *Optical nonlinearity enhancement of graded metal-dielectric composite films*, Europhys. Lett. **67**, 854 (2004)

IV. L. Dong, M. Karttunen, and K. W. Yu, *Spectral representation of the effective dielectric constant of graded composites*, Phy. Rev. E **72**, 016613 (2005).

V. L. Dong, J. P. Huang, K. W. Yu, and G. Q. Gu, *Multipole polarizability of a graded spherical particle*, Eur. Phys. J. B **48**, 439 (2005).

VI. J. P. Huang, L. Dong, and K. W. Yu, *Giant enhancement of optical nonlinearity in multilayer metallic films*, J. Appl. Phys. **99**, 053503 (2006).

VII. En-Bo Wei, L. Dong, and K. W. Yu, *Effective ac response of graded colloidal suspensions*, J. Appl. Phys. **99**, 054101 (2006).

In the overview these publications are referred to by their roman numerals.

Author's contribution

The author has had an active role in all the phases of the research reported in this thesis. She has participated in planning the research. She has developed all of the calculations and analysis of results reported in Publications I, II, IV and V, and some of the calculations and analysis of results reported in Publications III, VI and VII. She has written the the Publications I, II, IV and V, and has contributed actively to the writing of Publications III, VI and VII.

Additional publications of the author (not included in this thesis):

- L. Dong, G. Q. Gu, and K. W. Yu, *First-principles approach to dielectric response of graded spherical particles*, Phys. Rev. B **67**, 224205 (2003).
- J. P. Huang, M. Karttunen, K. W. Yu, and L. Dong, *Dielectrophoresis of charged colloidal suspensions*, Phys. Rev. E **67**, 021403 (2003).
- J. P. Huang, M. Karttunen, K. W. Yu, L. Dong, and G. Q. Gu, *Electrokinetic behavior of two touching inhomogeneous biological cells and colloidal particles: Effects of multipolar interactions*, Phys. Rev. E **69**, 051402 (2004).
- J. P. Huang, K. W. Yu, G. Q. Gu, M. Karttunen, and L. Dong, *Reply to "Comment on the use of the method of images for calculating electromagnetic responses of interacting spheres"*, Phys. Rev. E **72**, 023402 (2005).
- T. Róg, L. Stimson, L. Dong, A. Wisniewska, M. Dutka, and M. Karttunen, *Stearic acid spin labels in lipid bilayers: Insight through atomistic simulations*, J. Phys. Chem. B **111**, 12447, (2007).

Chapter 1

Introduction

1.1 Colloids

1.1.1 What are colloids

Colloids are heterogeneous systems in which one or more of the components has at least one dimension within the micrometer (10^{-6}m) range, i.e., it concerns systems containing large molecules or macroscopic particles. Familiar examples include industrial and household products such as paints and inks, food products such as mayonnaise and milk, and biological fluids such as biological molecules (e.g., erythrocytes) and viruses.

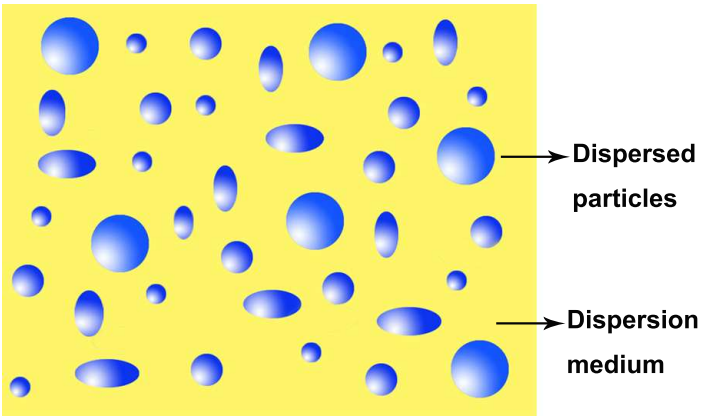

Figure 1.1: A schematic picture of a colloidal dispersion.

The most typical and common colloids are two-phase dispersions, i.e., dispersions of (Figure 1.1) finely divided particles with colloidal size dispersed in a

continuous medium of a different composition. The phases are distinguished as the *dispersed phase* (dispersed particles) and the *dispersion medium* (the continuous medium). Table 1.1 lists examples of some common types of such dispersions.

Examples	Term	Dispersed phase	Dispersion medium
Fog, clouds, smog, hairspray	Aerosol	Liquid	Gas
Smoke, dust, pollen	Aerosol	Solid	Gas
Lather, whipped cream, foam	Foam	Gas	Liquid
Milk	Emulsion	Liquid	Liquid
Ink, muddy water, paint	Sol	Solid	Liquid
Styrofoam, souffles	Porous solids foam	Gas	Solid
Butter	Solid emulsion	Liquid	Solid
Concrete	Solid suspension	Solid	Solid

Table 1.1: Some common colloidal dispersions classified by the dispersed phase and the matrix in which the particles are dispersed. Some of the systems are known by common names such as emulsions.

1.1.2 Historical view of colloids

Application of colloids can be traced back to the earliest records of civilization. Stone Age paintings in the Lascaux caves in France, and the pigments of Egyptian pharaohs were produced by stabilized colloidal pigments [1], in which carbon black is stabilized by gum arabic [2]. Many of our earliest technological processes, such as paper-making, pottery, and the fabrication of soaps and cosmetics, involved manipulation of colloidal systems [1]. During the Middle Ages artisans codified their knowledge and formed guilds that served as the prototypes of present-day professional organizations [2].

The establishment of colloid science as a scientific discipline can be traced back to the mid-nineteenth century. In 1847 Italian chemist Francesco Selmi (1817-1887) reported detailed studies on the preparation of "pseudosolutions" (the term *colloid* had not been coined yet) such as the pigment Prussian Blue (iron (III) hexacyanoferrate (II)), prepared by mixing solutions of potassiumferrocyanide and ferric chloride, or sulphur sols formed by the reaction of hydrogen sulfide with an aqueous solution of sulfur dioxide [3]. In the 1850s Michael Faraday (1791-1867) made extensive studies of colloidal gold sols, which involve solid gold particles suspended in water. He

described how to obtain colloidal gold as a red sol by treating chloroauric acid with a variety of reducing agents in his famous Bakerian Lecture on "*Experimental relations of gold (and other metals) to light*" [4]. He found that these sols can be stabilized kinetically. However, these stabilizations are thermodynamically unstable to coagulate because of the attraction between suspended particles. We know now that the attraction is just the van der Waals interaction. Once they have coagulated, the process can not be reversed. If properly prepared, however, they can exist for many years. In fact, some of the colloidal systems Faraday prepared are still on display in the British Museum in London [1].

In 1861 Thomas Graham (1805-1869) coined the term *colloid* (Greek *kolla* for glue) to describe Selmi's "pseudosolutions" [5]. The term emphasizes their low rate of diffusion and lack of crystallinity. At that time, Graham was studying the diffusion properties of various substances in solution, and aimed at distinguishing the substances which were capable of going through a wall of parchment from those which were not. He found that the substances which invariably exhibit a crystalline form in the pure state can penetrate the wall, however, those who can not penetrate the wall have a rather glutinous appearance. Graham deduced that the low diffusion rate of colloidal particles implied that they were fairly large – at least 1 μm in diameter in modern terms. On the other hand, the failure of the particles to sediment under influence of gravity implied that they had an upper size limit of approximately 1 nm. Graham's definition of the range of the particle size that characterize the colloidal domain is still widely used today.

1.1.3 Classification of colloids

Colloids are traditionally divided into two categories, *lyophilic* (liquid-loving) and *lyophobic* (liquid-hating), depending on their interaction with the dispersion medium. If the liquid medium is aqueous, the terms *hydrophilic* and *hydrophobic* are used. The lyophilic colloids are formed spontaneously when the substance (e.g. gelatin, rubber, soap) is brought in contact with the dispersion medium. Hence they are thermodynamically stable. Lyophobic colloids (e.g. gold sol) can not be formed by spontaneous dispersion in the medium. They are thermodynamically unstable with respect to macroscopic phase, but they may remain for long times in a metastable state.

Lyophilic colloids comprise both *association* colloids in which aggregates of small molecules are formed reversibly, and *macromolecules* in which the molecules themselves are of colloidal size.

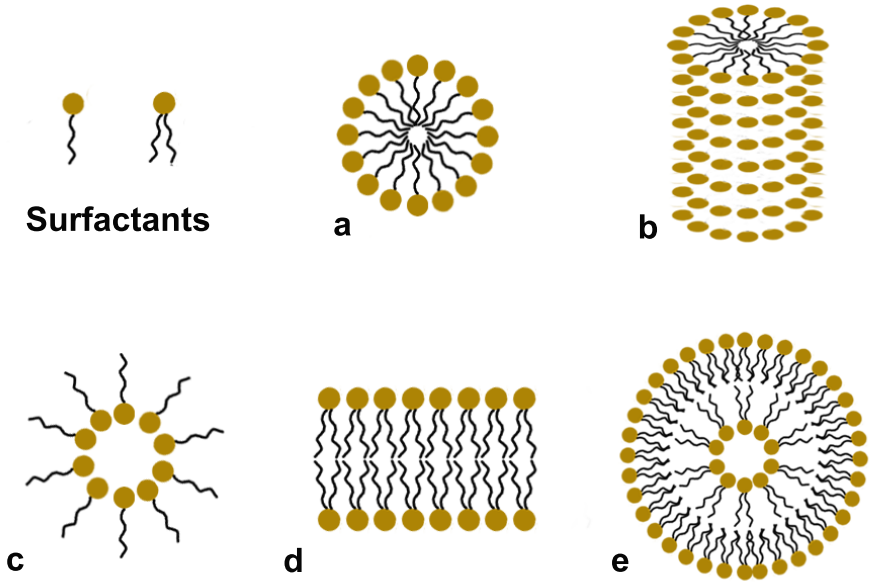

Figure 1.2: Typical aggregate morphologies into which surfactant self-assemble in aqueous solution (a) spherical micelle, (b) rod micelle, (c) inverted micelle, (d) bilayer fragment, and (e) vesicle.

Association colloids are typically formed by amphiphilic (both "oil and water-loving") molecules such as surfactants (Figure 1.2) and lipids, which consist of a hydrophobic and a hydrophilic part. They orientate their hydrophilic segments toward the solvent, while the other part of the molecule turns to avoid contacting with the solvent. As a result, amphiphilic molecules align according to well-defined patterns and give rise to colloidal aggregates such as micelles (Figure 1.2). Amphiphilic self-organizing systems are more complex than colloidal dispersions. One reason for this is that amphiphiles are associated physically [1], consequently, microstructural size and shape can change in response to subtle variations in concentration or temperature. This facile response to chang environmental conditions contrasts strongly with the relatively immutable behavior of colloidal sols.

Macromolecular colloid is another type of colloid. A polymer is one type of macromolecules. Polymer solutions exhibit many features of colloidal solutions, they form spontaneously and are thermodynamically stable. For

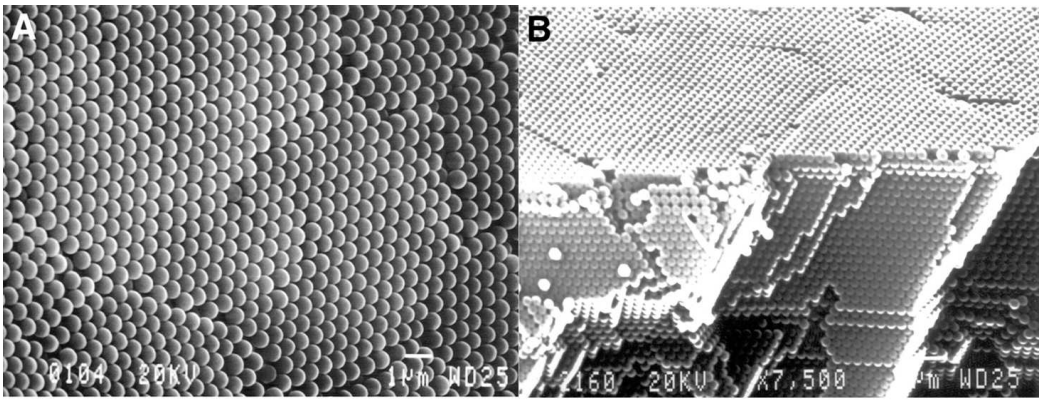

Figure 1.3: (A) A scanning electron micrograph of a typical area on the surface of the latex assembly; (B) A scanning electron micrograph along the edge of a broken particle. The surface is seen at the top and the cut through the bulk is toward the bottom of the micrograph. Scale bars, $1\mu m$ [6].

example, latex (Figure 1.3) is a colloidal sol formed by polymeric particles. They are easily prepared by emulsion polymerization, and the result is a nearly monodisperse suspension of colloidal sphere. Polymer solutions can be modified in a controlled manner to produce charge-stabilized colloids or by grafting polymer chains onto the particles to create a sterically stabilized dispersion, such as stabilization of black carbon absorbed by arabic gum.

1.1.4 Characteristic physical phenomena related to colloids

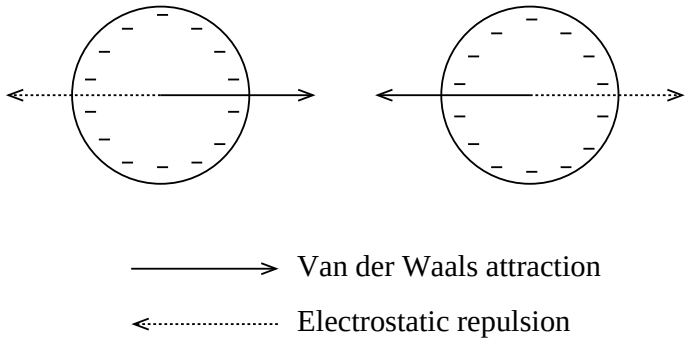

Figure 1.4: Stabilization of colloids by electrostatic forces. The attractive van der Waals force has its origin in atomic polarizabilities.

Neutral particles in a common solvent attract each other by van der Waals forces, resulting in clumping together, followed by the formation of sediment. How can this be avoided? One effective way is to change the surface of the dispersed particles, i.e., change the interface between the dispersed particle and dispersion medium. One of the characteristic features of colloidal suspension is large interface between particles. Grains, e.g., gold particles in water carry an electric charge (Figure 1.4) and repel each other by Coulomb forces. This force neutralizes the van der Waals attraction, and the gold grains remain isolated: the colloid is stabilized. This stabilization process was discovered by Faraday. If salt is added (sodium chloride), the charge surface of a dispersed grain is neutralized by the added ions, that is, the Coulomb repulsions are screened out and thus the system clumps (Figure 1.5). The optical characteristics of the suspension are altered. Red corresponds to absorption of light by individual gold grains; blue corresponds to a clumped system in which only negative chloride ions are left.

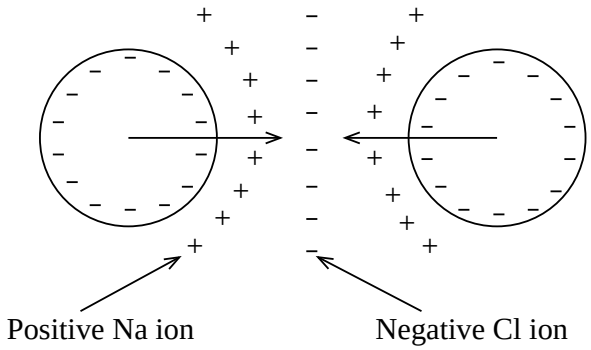

Figure 1.5: Inhibition of stabilization by dissolution of an ionic salt. The arrows denote the van der Waals attraction.

It is often difficult to keep water salt-free on an industrial scale, so colloids must be protected by other means. The scribes of ancient Egypt needed ink, which was based on carbon black mixed with water. But this two-component mixture was unstable: the carbon grains attracted each other by van der Waals forces, clumping together and forming a sediment within a few minutes. So the wise Egyptians added gum arabic (a polysaccharide obtained from the acacia tree). This is a long-chain polymer, which adsorbs onto the carbon grains, forming a 'halo' around each one. When two grains come close to each other, the halos overlap and create a repulsive force. The ink was thus stabilized, and would last for months. On the other hand, when wine is cloudy (due to some unwelcome fermentation), the winemaker carries out a clarification. This involves pouring watered-down egg white into the barrel,

whilst stirring it; the natural polymer causes organic particles in suspension to aggregate, forming agglomerates sufficiently large to be sedimented out. The clear wine is then decanted.

Colloids have another identifying property, an optical effect, which is referred to as the *Tyndall effect*, after British physicist John Tyndall (1820 -1893). This effect is caused by scattering of light by colloidal particles. When a relatively narrow beam of light is passed through a colloid, such as *dust* particles in the air, light is scattered by the dust particles and they appear in the beam as bright, tiny specks of light. The scattering of light in a colloid due to the reflection by large colloidal particles produces a visible beam of light. No observable reflection is caused by the smaller solute particles in a solution. Hence, a beam of light passing through a solution is invisible. The most famous phenomenon of Tyndall effect of colloids is that is impossible to see the beams of light from the car's headlights, when a driver encounters a foggy area on a highway at night.

1.1.5 Why are colloids interesting

Size of the colloids, time scale of their diffusion and tunable interactions make them as ideal tools for fundamental investigations [7]. For example, the discovery of Brownian motion resulted from observation of colloidal-sized pollen particles by light microscopy; Einstein developed the relationship between Brownian motion and diffusion coefficients. In 1909 Jean Baptiste Perrin (1870 -1942) used this relationship to determine Avogadro's number. Subsequently, Marian Smoluchowski (1872 - 1917) derived an expression that related to the kinetics of rapid coagulation of colloidal particles to the formation of a larger dimer particle. His expression was extended to explain the role of diffusion in biomolecular reactions in general.

In industrial applications, monodisperse colloidal particles with specific physical-chemical properties, adequate reactive groups, morphology and self-assembly capabilities are opening up many new applications and possibilities for making products such as magnetic drug carriers, bio-sensors, implants, magnetic resonance imaging (MRI), ceramics, coatings, new electronic, optoelectronic and magnetic devices. In particular, hybrid colloids with mixed structure, containing inorganic (e.g. iron-oxides, silica) and organic (e.g. polymers, chromophore or fluorophore, proteins) material, as well as colloids with complex morphology such as core-shell and non-spherical shapes, are attracting considerable technological interest due to their unique properties (catalytic,

magnetic, optical, mechanical, etc.), which differ from those of their atomic and bulk counterparts [8, 9].

1.2 Functionally graded materials

In this thesis, the suspended particles in the colloidal systems can be homogeneous as well as graded. The previous introduction is a general introduction about colloids, however, in the following section, we focus on graded colloidal particles. Such materials are often called as functionally graded materials (FGMs).

1.2.1 Definition and historical review

Functionally graded materials (FGMs) are heterogeneous since their properties or structures may vary continuously in space. For example, one side may have high thermal resistivity and the other side may have high mechanical strength, which means that two aspects are present in one material. There are many graded structures and functions in nature, such as bio-tissues of plants and animals, and even human bones and teeth.

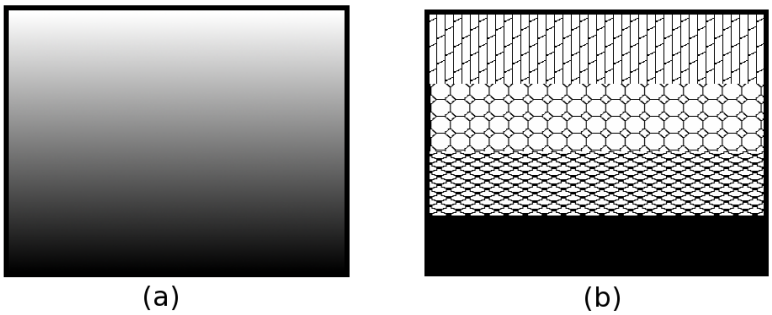

Figure 1.6: Structure of functionally graded materials. (a) shows continuous graded structure and (b) shows stepwise graded structure [10].

The simplest FGMs are two different material ingredients which either change gradually from one to the other as illustrated in Figure 1.6 (a), or change in a discontinuous way such as the stepwise gradation – graded thin film – illustrated in Figure 1.6 (b). One of well known FGMs is compositionally graded from a refractory ceramic to a metal. Such FGM is synthesized by two materials with different properties, such as the heat resistant ceramics with

metals which have high toughness and strength. The concept of the FGMs was first considered in Japan in 1984 during a space plane project, where a combination of materials would function as a thermal barrier capable of withstanding surface temperatures up to 2000 K and temperature gradients of 1000 K across a 10 mm section [11]. These materials received considerable attention as one of the advanced inhomogeneous composite materials and have been explored in various engineering applications since first being reported [11]. These materials can be tailored in their materials properties via the gradients. Benefits include the reduced residual and thermal barrier coatings of high temperature components in gas turbines, surface hardening for tribological protection and graded interlayers used in multilayered microelectronic and optoelectronic components [11–13].

1.2.2 Applications of functionally graded materials

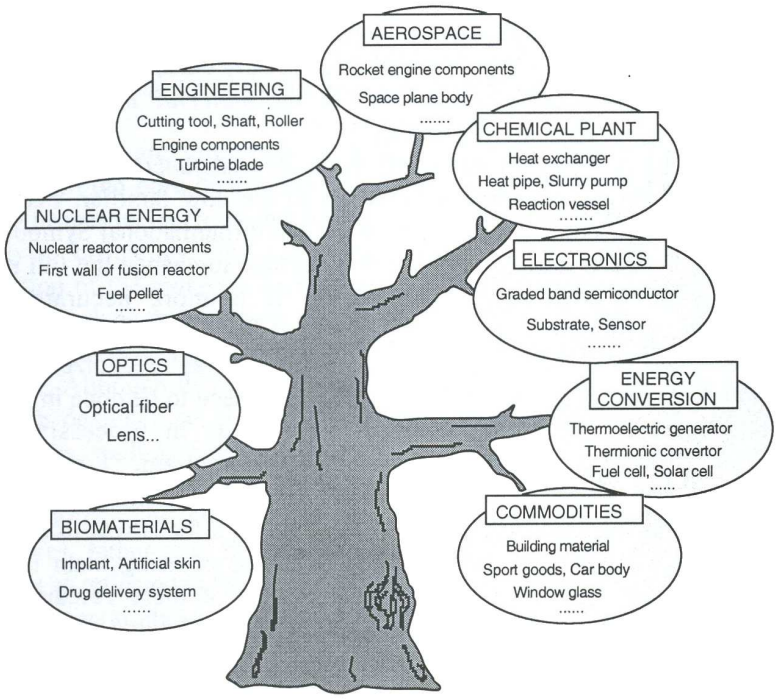

Figure 1.7: Potentially applicable fields for FGMs [10].

The concept of FGMs is applicable to many fields, as illustrated in Figure 1.7. It was originally devised in aeronautics, in which FGMs were to provide two

conflicting properties such as thermal conductivity and thermal barrier in one material. At present, they enable the production of light-weight, strong and durable materials, and they are applicable to a broad range of fields such as structural materials, energy conversion materials and so on. In particular, FGMs will be a vital technology for rocket and space stations.

In industrial applications, recent products for industrial tools are getting stiffer, which requires that the materials have both wear resistance and toughness. Hence, the application of FGMs is a possible solution. A trial production of an industrial tool for dry cutting has been successfully conducted using diamond (outside) and steel (inside).

Communication tools using optical fibers need further advancement, especially given the increasing volume of information. One idea is a light wavelength multiplex communication system using a refractive index graded fiber. The refractive index for wave transmitting direction continuously varies along with wavelength frequency. With a refractive index graded fiber, unnecessary refraction can be prevented to some extent. Application of FGMs to plastic optical fibers can provide high-speed transmission.

The application of FGMs in biomaterials is growing in importance. Over 2500 surgical operations to incorporate graded hip prostheses have been successfully performed in Japan over the past decade [10]. These graded hip implants enable a strong bond to develop between the titanium implant, bone cement, hydroxyapatite, and bone. The bone tissue penetrates hydroxyapatite granules inserted between the implant and the bone thus forming a graded structure.

1.2.3 Functionally graded films

Thin graded films are of great interest in many practical applications and often possess different optical properties in comparison to bulk materials [14]. Moreover, from the practical point of view, multilayer film materials are more convenient to fabricate than bulk graded materials [15] and, there are many algorithms available for designing multilayer coatings [16, 17].

1.3 Structure of this thesis

The objective of this thesis is to investigate dielectric properties such as effective dielectric constant and effective dipole factor of colloidal systems in

which the suspended particle can either be homogeneous or graded. The thesis presents the results of a series of theoretical and computational studies of different colloidal systems. Chapter 2 reviews the theories that have been used in this study to describe colloidal systems. As we are mostly interested in the dielectric properties of colloidal particles, we focus on properties such as polarization of particles subjected to external electric fields as well as their mutual electrostatic interactions. The latter becomes increasingly important when the density of the suspended particles increases, or when they aggregate due to, for example, exposure to an external field. Theories involving dielectrophoresis, nonlinear alternating current response and effective dielectric response are discussed in detail as they are among the main topics of the original research presented in this thesis.

In textbook scenarios, theories relate to ideal models. Real systems, however, should be modeled by considering the complexity of all these systems. For example, we can represent cells as uniform spheres in some systems, or we may represent them as multilayer sphere, or even as continuously graded spheres. Hence, Chapter 3 describes the models of our study. The Maxwell-Garnett theory is used to describe the dilute systems. By contrast, the effective medium theory is applied to study colloidal system with high concentration. The methods developed in this thesis, such as the first-principles approach and differential effective multipole moment approximation, are given in detail.

Finally, an overview of the results are given in Chapter 4. In addition, the publications are referred to, where appropriate, in the rest of the overview.

Chapter 2

Background

2.1 Polarization in materials

Macroscopic objects belong (at least, to a good approximation) to one of two large classes: *conductors* and *insulators* (or *dielectrics*). Conductors are substances that contain an "unlimited" supply of charges that are free to move through the material. In practice what this ordinarily means is that many of the electrons (one or two per atom in a typical metal) are not associated with any particular nucleus, but are free to roam around. In dielectrics, by contrast, all charges are attached to specific atoms or molecules, and hence, are restricted to limited motions about the specific atoms or molecules. Such microscopic displacements are not dramatic, but their cumulative effects account for the characteristic behaviors of dielectric materials.

What happens to a neutral atom when it is placed in an electric field $\mathbf{E}_0$? Your first guess might well be:"Absolutely nothing, since the atom is not charged, the field has no effect on it." But this is incorrect. Although the atom as a whole is electrically neutral, there is a positively charged core (the nucleus) and a negatively charged electron cloud surrounding it. These two regions of charge within the atom are influenced by the field: the nucleus is pushed in the direction of the field, and the electrons the opposite way. In principle, if the field is large enough, it can pull the atom apart completely, "ionizing" it (the substance then becomes a conductor). For smaller fields, however, the center of the electron clouds is shifted away from the nuclear position resulting in an effective attractive interaction between the electrons and nucleus, and this holds the atom together. The two opposing forces,

which are $\mathbf{E}_0$ pulling the electrons and nucleus apart and their mutual attraction drawing them together, eventually reach equilibrium. As a result, the atom is *polarized*, (Figure 2.1) with positive charge and negative charge regions. The atom now has a tiny dipole moment $\mathbf{p}$, which points in the same direction as $\mathbf{E_0}$. Typically, this induced dipole moment is proportional to the field:

$$\mathbf{p} = \alpha \mathbf{E}_0. \tag{2.1}$$

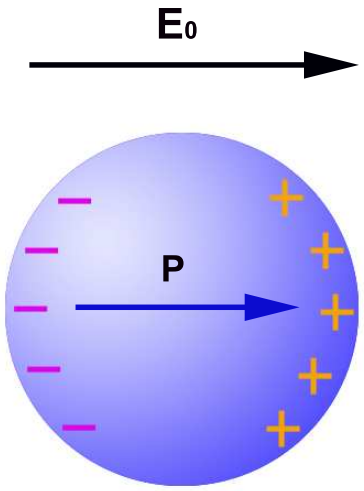

Figure 2.1: Dielectric sphere in a uniform field $\mathbf{E}_0(\mathbf{r})$, showing the polarization charge which forms the dipole. $\mathbf{p}$ is the dipole moment induced by the applied electric field.

The constant of proportionality α is called *atomic polarizability*. Its value depends on the detailed structure of the atom in question.

The neutral atom has no dipole moment to start with — $\mathbf{p}$ was induced by the applied field. Some molecules, called *polar molecules*, have built-in, permanent dipole moments. In the water molecule (Figure 2.2), for example, the electrons tend to cluster around the oxygen atom, and since the molecule is bent at 105°, this leaves a negative charge at the vertex and a net positive charge at the opposite end, which forms the dipole $\mathbf{p}$. (The dipole moment

of water is usually large: $6.1 \times 10^{-30}\mathrm{C} \cdot \mathrm{m}$; in fact this is what accounts for its effectiveness as a solvent.) When such a molecule is placed in an electric field, there will be a torque tending to line it up along the direction of the field.

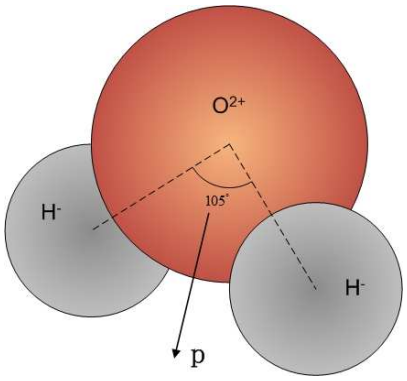

Figure 2.2: Water molecule with its permanent dipole.

These two mechanisms produce the same basic result: a lot of little dipoles pointing along the direction of the field, thus the materials becomes *polarized*. A convenient measure of this effect is

$$\mathbf{P}(\mathbf{r}) = \sum_i N_i \langle \mathbf{p}_i \rangle, \tag{2.2}$$

which is called *polarization*, and $\mathbf{p}_i$ is the dipole moment of the ith type of molecule in the medium, the average is taken over a small volume centered at $\mathbf{r}$ and N_i is the average number per unit volume of the ith type of molecule at the point $\mathbf{r}$.

Polarization in materials can be due to several mechanisms: electronic (atomic), ionic, molecular (dipole), and interfacial (space-charge) polarization [19–21]. The effect on each mechanism can be seen schematically in Figure 2.3. For a given material, the sum of contributions from each mechanism determines the net polarization, $\mathbf{P}$, of the dielectric material,

$$\mathbf{P} = \mathbf{P}_{electronic} + \mathbf{P}_{ionic} + \mathbf{P}_{molecular} + \mathbf{P}_{interfacial}. \tag{2.3}$$

Electronic polarization exists in all materials and is the response of the electrons and the atomic nuclei that shift their relative positions under an applied electric field and form an electric dipole (each per atom or ion). This polarization occurs instantaneously, in response to light electromagnetic field frequency ($\sim 10^{15}$ Hz), since the electrons have a very high natural frequency

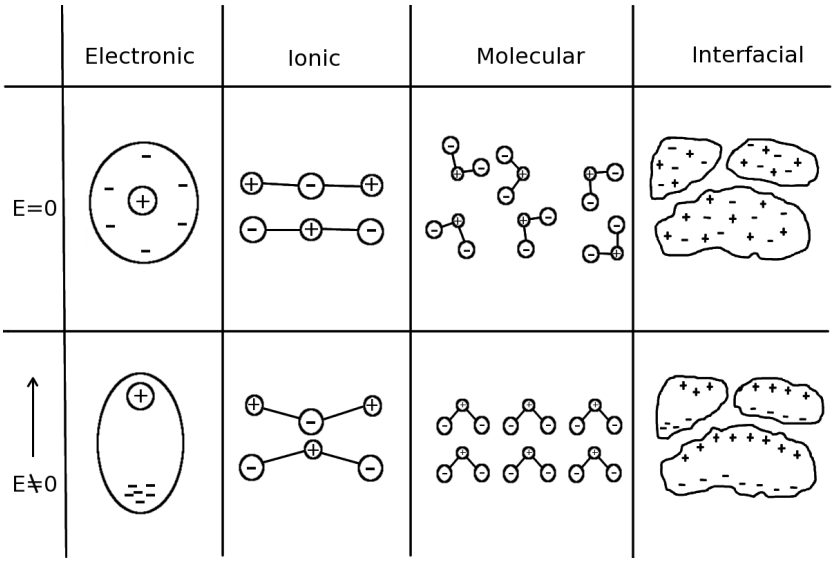

Figure 2.3: Polarization mechanisms [18]

($\sim 10^{16}$ Hz). Ionic polarization is the displacement of negative and positive ions toward the positive and negative electrodes, respectively. Since they are much more massive than electrons, the ions cannot become polarized as rapidly. Ionic polarization is limited to maximum frequency of approximately 10^{13} Hz. Molecular polarization occurs in materials consisting of polar molecules (or unit cells) only. The maximum frequency of response varies significantly from material to material depending on the size of molecules, but is always less than that for electronic and ionic polarization and is typically less than 10^{10} Hz. Interfacial polarization is a short-range electric conduction process. Due to the nature of diffusion, space charge polarization occurs rather slowly and the typical frequency of response is approximately 10^2 Hz. Figure 2.4 summarizes the frequency dependence of various polarization mechanisms.

2.1.1 Dielectric constant

For many substances, polarization is proportional to the field, provided $\mathbf{E_0}$ is not too strong,

$$\mathbf{P} = \epsilon_0 \chi_e \mathbf{E}. \tag{2.4}$$

This constant of proportionality, χ_e, is called the *electric susceptibility* of the medium, ϵ_0 is the permittivity of vacuum. Materials that obey Equation (2.4) are called *linear dielectrics*. Note that $\mathbf{E}$ is the total field — macroscopic

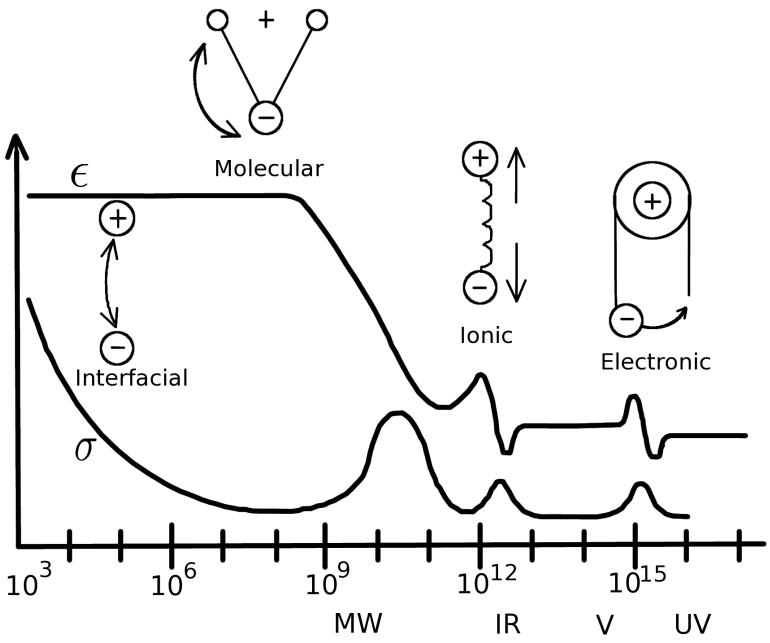

Figure 2.4: Frequency response of dielectric mechanisms [22].

electric field; it may be due in part to free charges and in part to polarization itself. With the definition of displacement $\mathbf{D} = \epsilon_0\mathbf{E} + \mathbf{P}$, we have

$$\mathbf{D} = \epsilon_0\mathbf{E} + \epsilon_0\chi_e\mathbf{E} = \epsilon_0(1 + \chi_e)\mathbf{E}, \tag{2.5}$$

so $\mathbf{D}$ is also proportional to $\mathbf{E}$:

$$\mathbf{D} = \epsilon\mathbf{E}, \tag{2.6}$$

where

$$\epsilon = \epsilon_0(1 + \chi_e) \tag{2.7}$$

is the permittivity of the material.

$$\epsilon_r = \frac{\epsilon}{\epsilon_0} = (1 + \chi_e) \tag{2.8}$$

is called the *relative permittivity* of the material. Table 2.1 shows examples of this parameter.

2.1.2 Complex dielectric constant

Poisson's equation is used to describe the electrostatic properties of the materials. For nonconducting medium, Poisson's equation is given by

$$\nabla \cdot (\epsilon\nabla\Phi) = -\rho, \tag{2.9}$$

Material	Dielectric constant	Material	Dielectric constant
Vacuum	1	Benzene	2.28
Helium	1.000065	Diamond	5.7
Neon	1.00013	Salt	5.9
Hydrogen	1.00025	Silicon	11.8
Argon	1.00052	Methanol	33.0
Air (dry)	1.00054	Water	80.1
Nitrogen	1.00055	Ice(-30°C)	99
Water vapor (100°C)	1.00587	$KTaNbO_3$(0°C)	34,000

Table 2.1: Relative permittivity (unless otherwise specified, values given are for 1 atm, 20°C). Source: Handbook of chemistry and physics, 78th ed. (Boca Raton: CRC Press, Inc., 1997).

where Φ and ρ denote the electrical potential and charge density in the considered region, respectively. For a conductive medium with conductivity σ, no free charges and sources are allowed, and the Poisson's equation is given by

$$\nabla \cdot (\sigma \nabla \Phi) = 0. \tag{2.10}$$

When the medium is a mixture of these two cases (a lossy dielectric), it consists of dielectric and conductive components. The Poisson's equation then becomes time dependent, and is given by a complex electric potential in the region with the coupling of Equations (2.9) and (2.10), which is also known as the continuity equation for the current density

$$\nabla \cdot (\sigma \nabla \Phi) + \frac{\partial}{\partial t} \nabla \cdot (\epsilon \nabla \Phi) = 0. \tag{2.11}$$

Equivalently, Equation (2.11) can be written as

$$\nabla \cdot (i\omega \tilde{\epsilon} \nabla \Phi) = 0, \tag{2.12}$$

where $\omega = 2\pi f$ being the angular frequency of the external electric field, $i = \sqrt{-1}$, and $\tilde{\epsilon}$ is the *complex dielectric constant* defined as

$$\tilde{\epsilon} = \epsilon + \frac{\sigma}{i\omega}. \tag{2.13}$$

The significant factor regarding complex dielectric constant is that it is frequency dependent (i.e., it contains an ω term). If we consider the behavior of Equation (2.13) at very high frequencies ($\omega \to \infty$), the imaginary term tends to zero and $\tilde{\epsilon}$ is dominated by the permittivity. At very low frequencies

($\omega \to 0$), conductivity term becomes very large and dominates over permittivity. Therefore, there are two types of behavior — permittivity dominated and conductivity dominated. At intermediate frequency there is a crossover region from one type of behavior to another.

2.2 Dielectric spherical particles in electric field

When a polarizable particle suspended in another medium is exposed to an electric field, charge builds up at the interface between the surface of the particle and its surroundings; differences in the numbers of positive and negative charges accumulating on the surface mean that the particle is polarized. Since any electrostatic interaction with the particle can be treated as if it were an interaction with the dipole across the particle, we can determine the behavior of the particle by determining the dipole.

If an electric field $\mathbf{E}_0$ is applied to a polarizable particle, then charge accumulates at opposite surfaces of the particle along the field vector to form a dipole. However, if the particle contains no excess charge (i.e., it is charge neutral), then the solution of Equation (2.10) in spherical coordinates lead to a uniform electric field within in the particle [23]),

$$\mathbf{E} = \frac{3\epsilon_2 \mathbf{E_0}}{\tilde{\epsilon}_1 + 2\tilde{\epsilon}_2}, \tag{2.14}$$

where subscripts 1 and 2 refer to the particle (inside the body) and medium (outside the body), respectively.

The induced polarization $\mathbf{P}$ per unit volume within the particle is given by the expression

$$\mathbf{P} = (\tilde{\epsilon}_1 - \tilde{\epsilon}_2)\mathbf{E}. \tag{2.15}$$

Therefore, the dipole moment for a sphere of radius a is given by

$$\mathbf{p} = \frac{4}{3}\pi a^3 \mathbf{P}. \tag{2.16}$$

From this, the induced dipole moment for a spherical particle suspended in electric field can be written as

$$\mathbf{p} = 4\pi a^3 \epsilon_2 \frac{\tilde{\epsilon}_1 - \tilde{\epsilon}_2}{\tilde{\epsilon}_1 + 2\tilde{\epsilon}_2} \mathbf{E_0}, \tag{2.17}$$

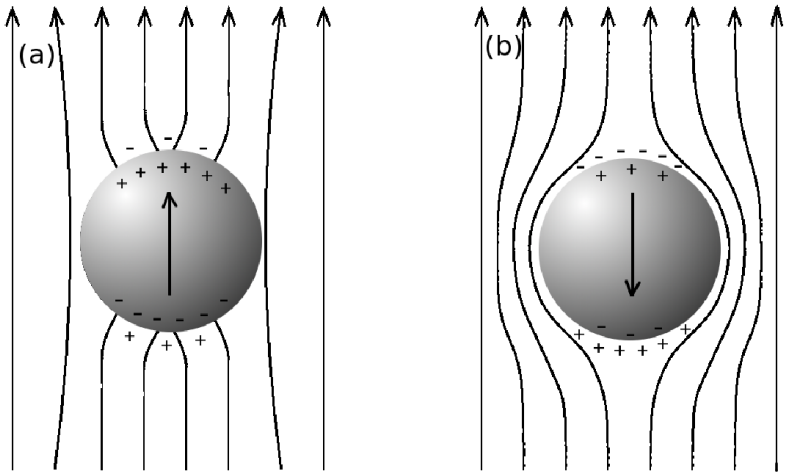

Figure 2.5: (a) If the particle is more polarized than medium, the induced electric field is aligned to counter the external field, and the field is warped toward the particle (and intersects the conducting surface at right angles). (b) If the particle is less polarized than medium, the dipole is oriented in the opposite direction of the external field and the field lines wrap around the particle.

where the bracketed term is the referred to as the Clausius-Mossotti factor or dipole factor, b

$$b = \frac{\tilde{\epsilon}_1 - \tilde{\epsilon}_2}{\tilde{\epsilon}_1 + 2\tilde{\epsilon}_2}. \tag{2.18}$$

This describes the dipole moment for a spherical dielectric particle suspended in a dielectric medium; note that $\mathbf{p}$ depends on the dielectric properties of both particle and medium and can change sign according to the complex dielectric constants of the particle and medium. In the situation, where the particle is more polarizable than the medium, impedance is dominated by conduction in the particle and capacitance in the medium, and a larger amount of charge will accumulate on the medium side of the interface (which is acting like a capacitor) than on the particle side (which is acting like a conductor). The imbalance between the charges means that across the particle as a whole (including the charge on the interface) there is a dipole oriented along the electric field (Figure 2.5(a)). If the medium is more conductive than the particle, then there will be more charge on the particle side of the interface than on the medium side, and hence the net dipole is oriented opposite the field (Figure 2.5(b)). Where the complex dielectric constant of the particle and medium are equal, the net charge is zero and no dipole is

present.

2.3 Electrokinetics

As we mentioned in Section 1.1.2, when colloidal particles disperse into a continuous medium, they are normally charged; on the other hand, if the colloidal system is subject to an external electrical field, electric fields can have a profound effect on the flow behavior of the dispersion. This gives rise to electrokinetics – manipulation by controlling the electrostatic interactions between particles and their environment. For example, electrophoresis, dielectrophoresis (DEP), elecrorotation (ER), and traveling-wave dielectrophoresis (traveling-wave DEP) are specific application forms of electrokinetics. The best known of these effects is electrophoresis, a force imparted on a charged particle due to the attraction between the electrode and the charges on the particle, causing the particle to move toward the electrode of opposite polarity. Electrophoresis was developed in the late 1930s by Arne Tiselius [24] of Uppsala University in Sweden for the physical separation of colloidal mixtures and later proteins; he was awarded the Nobel Prize for chemistry for this in 1948. The principle of electrophoresis is that charged particles move through a non-moving liquid in a electric field at a speed proportional to their size and electrical charge, although typically one selects separation to be principally dictated by one or the other by careful choice of experimental conditions (such as pH and medium viscosity). Controlled electrophoresis experiments require the application of an electric field magnitude, known as a direct-current (DC) electric field, such that particles maintain a constant velocity independent of time or position on the matrix.

Electrophoresis is an important method used to separate biological particles such as proteins and DNA. Their differences in size, binding affinity and solubility determine the different moving velocity in the electrical field. It operates best on larger scales such as the now-famous stripes of DNA electrophoresis gels commonly used in medicine and forensic science for the determination of identity.

The second of these electrokinetic forces, known as *dielectrophoresis*, is the translational motion of particles induced by polarization effects in non-uniform electric field (Figure 2.6), described in some detail in texts by Pohl [25], Jones [26], and Zimmermann and Neil [27]. Certain types of particle, when subjected to an electric field, will polarize, the inherent charges separate and form a dipole. The poles interact with the electric field and generate electrostatic forces. If the field is non-uniform, the greater electric field strength

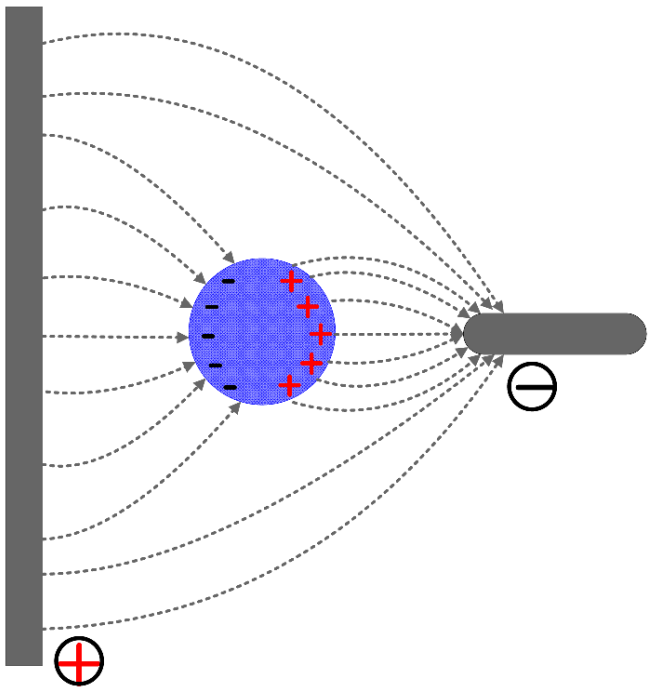

Figure 2.6: A schematic of a polarizable particle suspended within a point-plane electrode system. When the particle polarizes, the interaction between the dipolar charges with the local electric field produces a force.

across one side of the particle means that the force generated on that side is greater than the force induced on the opposing side of the particle and a net force is exerted toward the region of highest electric field. Moreover, this force will act toward the region of greatest electric field regardless of the orientation of the electric field and will thus also be present when an AC electric field is applied between the electrodes. This motion of the particles is termed *positive DEP*. However, if the particle is suspended in a medium more polarizable than itself, the electric field will be distorted around the particle, the induced dipole will orient in the opposite direction, and the force on the particle will be directed away from the high-field regions toward the low-field regions. This motion is referred to as *negative DEP*. The polarizability of the particle and medium is dependent on the frequency of the electric field, and it is possible for a particle to experience either positive DEP or negative DEP according to the frequency of the applied electric field. This is because the orientation of the dipole depends largely on the accumulation of charge on either side of the particle-medium interface (called a Maxwell-Wagner interfacial polarization). The relative amount of charge accumulated

depends on the impedance of these materials and hence the frequency of the applied field. As frequency changes, the relative dielectric behavior of the particle and medium change; in a given frequency window (called dielectric dispersion), the net behavior of the system changes from being dominated by the particle to being dominated by the medium, and the particles goes from experiencing positive DEP to experiencing negative DEP, that is, the force exerted on the particles changes sign on either side of one special frequency – crossover frequency.

There are a number of early observations of the DEP force; among the first experimental observations of the motion of particles in non-uniform electric fields were undertaken by Hatschek and Thorne [28] in the study of nickel suspended in toluene and benzene. The phenomenon was named DEP by Herbert Pohl in 1951 [29], who later published an in-depth treatise on the subject in his 1978 book *Dielectrophoresis*. Pohl's work advanced the use of DEP for investigating the properties of suspensions and for providing a means of separating particles from suspension. Similar investigations have been conducted using a frequency-based examination of DEP response of populations of cells (e.g., Gascoyne *et al.* [30] and Kaler and Jones [31]), yeast (e.g., Pohl and Hawk [32] and Huang *et al.* [33]), and bacteria (e.g., Hughes and Morgan [34]), including work by Nobel laureate Albert Szent-Györgyi. Practical applications of DEP have included the collection of cells for cellular fusion in biological experiments [35–37]. An other example of DEP is the separation of a mixture of two populations of latex beads, identical except for having different radii. Since the effective conductivity, which influences the polarizability of particles, of a latex sphere is dependent on the radius of particle, their crossover frequencies are different, which determines the force exerted on the particles. Therefore, between the crossover frequencies, particles exhibit different dielectrophoretic behavior – one experiences positive DEP, the other negative DEP – and can thus be separated.

Positive and negative DEP have been used to separate mixtures of viable and nonviable yeast cell [32, 38] and mixtures of healthy and leukemic blood cell [39]. Work by Rousselet *et al.* [40] and others applied DEP to the induction of continuous linear motion of particles, expanding on the basic concept of DEP as a means of trapping particles in a specific region in space. An important class of electrokinetic particle manipulator is the levitator – a device used to propel a particle against gravity, resulting the particle hovering in midsolution (or midair) at a height governed by its dielectric properties, allowing those properties to be measured, and allowing those particles to be selected and trapped [41, 42]. Early experiments used electric fields generated by (relatively) large electrodes and high voltages to trap particles (as

described by Pohl [25]); more recently, electrode structures have been fabricated using techniques borrowed from the computer industry (e.g., Huang, *et al.* [33], Markx and Pething [38], and Rousselet *et al.* [40]) to manipulate much smaller particles at much lower voltage.

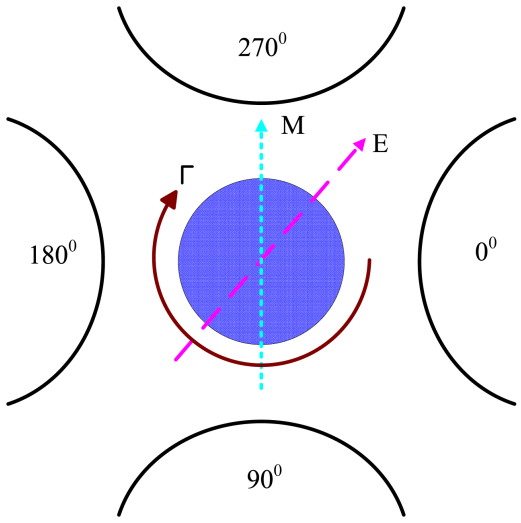

Figure 2.7: Electrorotation: a schematic of a polarisable particle suspended in a rotating electric field generated by four electrodes with 90 ° advancing phase.

Another form of electrokinetics is *electrorotation* (ER), the continuous rotation of particles suspended within rotating electric field (Figure 2.7); although this phenomenon produces quite different particle behavior than DEP, the two are closely related in origin [43, 44]. Cell rotation was observed and reported by experiments using alternative current DEP (e.g., Teixeira-Pinto *et al.* [45]) and was later suggested to be the result of the dipole-dipole interaction between neighboring cells [46]. This led Arnold and Zimmermann [47] to the principle of suspending single particles in a rotating field and thus to more amenable means of studying the phenomenon. ER occurs when a dipole is induced by a rotating electric field. Since the dipole takes a finite time to form, there is a time delay in the reorientation of dipole moment towards the direction of the electric field. The relative orientation between the applied electric field and the induced dipole induces a torque that rotates

the cell. The direction of rotation is determined by the angle between the dipole moment and the electric field; if the phase lag is less than 180^0, the particle rotation will follow that of the applied field, referred to as cofield rotation. If the phase angle is greater than 180^0, the shortest way in which the dipole can align with the electric field is by rotating in the opposite direction of the electric field (antifield rotation). As with DEP, the rate and direction of cell rotation are related to the dielectric properties of both the particle and the suspending medium. The technique thus can be used as an investigative technique for studying these properties. ER has been used to study the dielectric properties of matter, such as the interior properties of biological cells and biofilms (e.g.,Arnold and Zimmermann [48] and Zhou *et al.* [49]). A DC version (called Quinke rotation [26]) does exist; however, this is far more likely to be observed as a result of other work than specifically used for analysis.

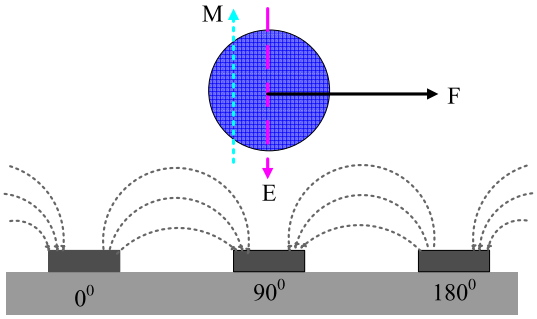

Figure 2.8: Traveling-wave dielectrophoresis: A schematic showing a polarizable particle suspended in a traveling electric field generated by electrodes on which the applied potential is 90 ° phase-advanced with respect to the electrode to its left. If the electric field E moves sufficiently quickly, the included dipole M will lag behind the electric field, inducing a force F in the particle. This causes the particle to move along the electrodes.

Yet another example of electrokinetics is *traveling-wave dielectrophoresis* (Figure 2.8). The phenomenon was first reported by Batchelder [50] and subsequently by Masuda *et al.* [51, 52], where the electric fields travel along a series of bar-shaped electrodes where low frequency (0.1 Hz to 100 Hz) sinusoidal potentials, advanced 120^0 for each successive electrode, were applied. This was found to induce controlled translational motion in lycopodium particles [52] and red blood cells [44]. At low frequencies, the translational force was largely electrophoretic, and it was proposed that such traveling fields could eventually find application in the separation of particles according to their size or electrical charge. However, later work by Fuhr and co-

worker [53], using applied traveling fields at much higher frequency ranges (10 kHz to 30MHz), demonstrated the induced linear motion in pollen and cellulose particles and also demonstrated that the mechanism inducing traveling motion at these higher frequencies is dielectrophoretic, rather than electrophoretic, in origin. Since then, Huang *et al.* [54] and others have, for example, used traveling fields to move yeast cells and separate them from a heterogeneous population of yeast and bacteria.

Traveling-wave DEP is effectively an extension of the principle of ER to the case of linear translation of electric field. An AC electric field is generated that travels linearly along a series of electrodes. Particles suspended within the field establish dipoles that, due to the relaxation time, are displaced from the regions of high electric fields. This induces a force in the piratical as the dipole moves to align with the field. If the dipole lags within half a cycle of the applied field, net motion acts in the direction of the applied field, while a lag greater than this results in motion counter to the applied field.

2.3.1 Dielectrophoresis

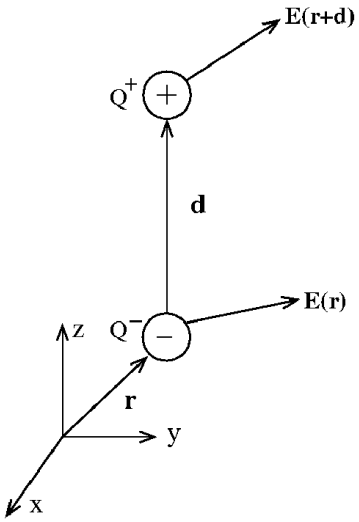

Figure 2.9: A schematic representation of the force exerted on a dipole in a nonuniform electric field.

One of the main topics of this thesis is dielectrophoresis and hence we will now describe it in detail. Let us consider a spherical particle with radius a in a nonuniform field $\mathbf{E}(\mathbf{r})$ such as the one shown in Figure 2.6. When this

particle polarizes, it will have centers of positive Q^+ and negative charges Q^- that are equal in magnitude Q but separated by a distance $\mathbf{d}$ along vector $\mathbf{r}$ as shown in Figure 2.9(a). Since the electric field is nonuniform, positive and negative charges will experience different electric field strengths. That gives rise to a net force on the particle of

$$\mathbf{F} = Q^+\mathbf{E}(\mathbf{r}+\mathbf{d}) - Q^-\mathbf{E}(\mathbf{r}), \tag{2.19}$$

where $\mathbf{d}$ is small relative to the size of the electric field nonuniformly. It can be approximated as

$$\mathbf{E}(\mathbf{r}+\mathbf{d}) = \mathbf{E}(\mathbf{r}) + \mathbf{d}\cdot\nabla\mathbf{E}(\mathbf{r}). \tag{2.20}$$

Thus, the force can be rewritten as

$$\mathbf{F} = Q\mathbf{d}\cdot\nabla\mathbf{E}. \tag{2.21}$$

Since $Q\mathbf{d}$ defines the dipole moment $\mathbf{p}$, the force can be written as

$$\mathbf{F} = (\mathbf{p}\cdot\nabla)\mathbf{E}. \tag{2.22}$$

In order to proceed further, we need to consider the nature of the electric field in a more realistic manner, that is, the fact that it may be changing either in space (having a magnitude gradient) or time (having a phrase gradient). The best example is the AC electric field which varies in three dimensions. This variation can be in the magnitude of the wave (the amplitude of the sine wave varies according to position), phase (the sine wave reaches its maximum at different times according to position), or both.

From Equation (2.17), the force on the particle can be derived,

$$\mathbf{F} = 4\pi a^3\epsilon_2\mathrm{Re[b]}(\mathbf{E}\cdot\nabla)\mathbf{E}, \tag{2.23}$$

where Re$[\cdots]$ denotes the real part of $[\cdots]$. Using the vector formula

$$\nabla(\mathbf{E}\cdot\mathbf{E}) = 2(\mathbf{E}\cdot\nabla)\mathbf{E} + 2\mathbf{E}\times(\nabla\times\mathbf{E}), \tag{2.24}$$

and $\nabla\times\mathbf{E} = 0$, the force thus can be written as

$$\mathbf{F} = 2\pi a^3\epsilon_2\mathrm{Re[b]}\nabla(\mathbf{E}\cdot\mathbf{E}). \tag{2.25}$$

The time-averaged force $\mathbf{F}_{\mathrm{DEP}}$ is given by

$$\mathbf{F}_{\mathrm{DEP}} = 2\pi a^3\epsilon_2\mathrm{Re[b]}\nabla\mathrm{E}^2_{\mathrm{rms}}, \tag{2.26}$$

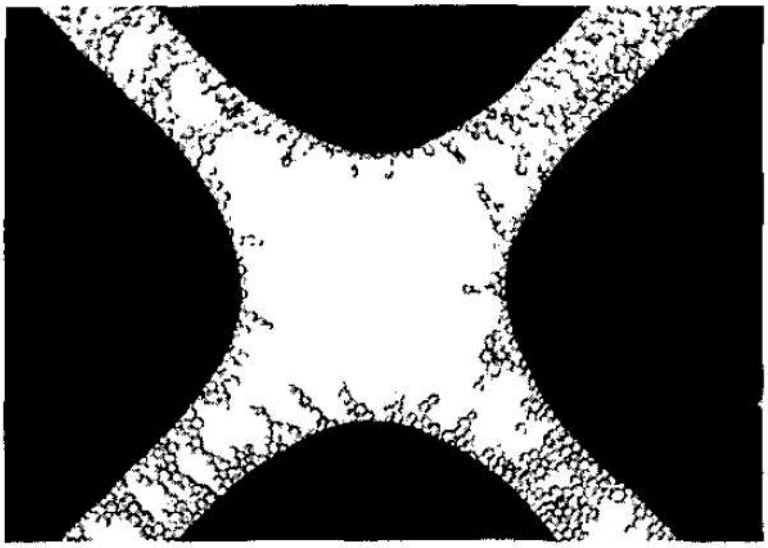

Figure 2.10: Positive dielectrophoretic collection of yeast cells suspended in 280 mM mannitol of conductivity 3.61 pS cm^{-1}, with 10 kHz, 10 V peak-peak signal applied to electrodes. Source: Electrode design for negative dielectrophoresis [55].

where E_{rms} is the root mean square magnitude of the imposed AC electric field.

One important feature to note is the fact that the expression for dielectrophoretic force contains the Clausius-Mossotti factor, which can take both positive and negative values. This has implications for the direction of the force; since $\mathbf{F}_{DEP}$ is a vector quantity, a change in sign will result in a change of direction. This property has been widely used to manipulate different particles. If Re[b] is positive, then the force acts in the direction of the increasing field gradient and hence moves toward the region of the highest electric field. This is so-called *positive dielectrophoresis* as shown in Figure 2.10 [55]. However, if the value of Re[b] is negative, then the value of the force is negative and the particle is repelled from the regions of a high electric field as shown in Figure 2.11 [55]. This is referred to as *negative dielectrophoresis*.

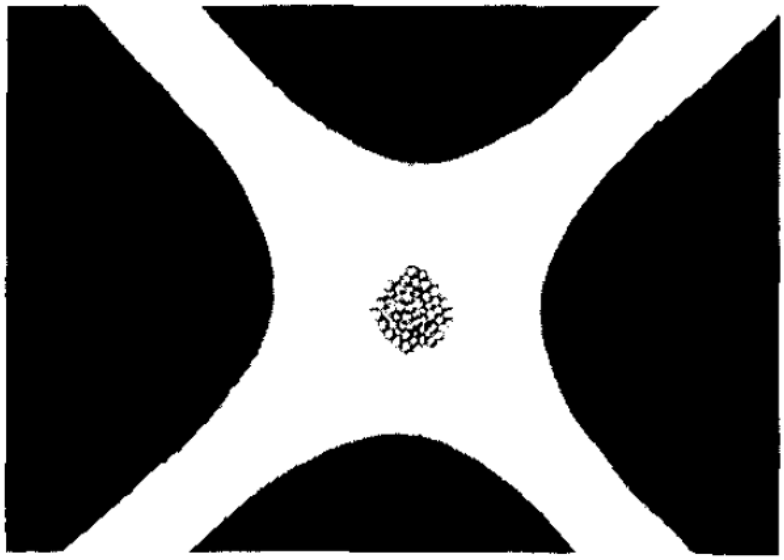

Figure 2.11: Negative dielectrophoretic collection of the same yeast cells as shown in Figure 2.10, when suspended in a 280 mM mannitol + 1.4 mM KCI solution of Conductivity 170 μS cm^{-1} and subjected to a 10 kHz, 10 V peak-peak signal applied to the electrodes. Source: Electrode design for negative dielectrophoresis [55].

2.4 Optical nonlinearity enhancement of graded composites

Optical nonlinearities have fascinated physicists for many decades because of the variety of intriguing phenomena that they display, such as frequency mixing and optical solitons [56, 57]. Moreover, they enable numerous important applications such as higher-harmonic generation, optical signal processing and ultrafast optical switches [57–59]. Composites are of particular interest because their nonlinearities may be strongly enhanced relative to bulk samples of the same materials. Various composite materials have been studied with respect to their nonlinear-optical properties such as metals or semiconductors in amorphous hosts — glass, plastic, or liquid [60, 61]. The physical origin of this enhancement is not conclusively known. For sufficiently small particles, quantum size effects [62, 63] or excitonlike confinement effects [64] help to increase the third-order optical susceptibility $\chi^{(3)}$ [65–69]. But even if such quantum size effects are unimportant, $\chi^{(3)}$ can still be enhanced by a purely classical effect, that is, the electric field within the particles is greatly

increased at optical frequencies because the composite is inhomogeneous. Such a field enhancement can be produced by an appropriate ratio of host-to-particle permittivity, by a modification of the field within a given particle by other neighboring particles, by anomalous dispersion, or by some combination of these effects.

In this thesis, the multilayer effect on the effective nonlinear optical response is discussed. We consider a graded metallic film with width L, and its gradation in the direction perpendicular to the film. The nonlinear characteristics are due to the field-dependence of the dielectric constant of the composite materials, which have a constitutive relation

$$\mathbf{D} = \epsilon(z,\omega)\mathbf{E}(z,\omega) + \chi^{(3)}(z,\omega)\left|\mathbf{E}(z,\omega)\right|^2\mathbf{E}(z,\omega), \tag{2.27}$$

where $\epsilon(z,\omega)$ and $\chi^{(3)}(z,\omega)$ are the linear dielectric constant and the third-order nonlinear susceptibility of the materials respectively. For convenience, we simplify $\chi^{(3)}(z,\omega)$ as $\chi(z,\omega)$. Because of this, composite materials are considered to prossess inversion symmetry, thus the second-order nonlinear optical response vanishes. Here, we also assume that the weak nonlinearity condition is satisfied, that is, the contribution of the third-order nonlinear effect is much less than that of the linear effect. Further, the discussion is restricted to the quasistatic approximation, under which the whole layered geometry can be regarded as an effective homogeneous one with effective (overall) linear dielectric constant $\bar{\epsilon}(\omega)$ and effective (overall) third-order nonlinear susceptibility $\bar{\chi}(\omega)$. With the above restrictions, the effective displacement can be given as [70]

$$\langle\mathbf{D}\rangle = \bar{\epsilon}(\omega)\mathbf{E}_0 + \bar{\chi}(\omega)\left|\mathbf{E}_0\right|^2\mathbf{E}_0, \tag{2.28}$$

where $\langle\cdots\rangle$ denotes the spatial average, and $\mathbf{E}_0 = E_0\hat{e}_z$ is the applied field along the z axis.

In this thesis we consider a bulk composite, that is, a small graded sperical metal particle embedded in an insulating matrix of dielectric constant of value unity. Then, the dielectric profile of the small graded spherical metal is given by the Drude expression

$$\epsilon(z,\omega) = 1 - \frac{\omega_p^2(z)}{\omega[\omega + i\gamma(z)]}, \quad 0 \le z \le L, \tag{2.29}$$

where the various plasma-frequency gradation profile is given by

$$\omega_p = \omega_p(0)(1 - C_\omega z), \tag{2.30}$$

and the relaxation-rate gradation profile [71] is

$$\gamma(z) = \gamma(\infty) + \frac{C_\gamma}{z}, \tag{2.31}$$

where C_ω is a dimensionless constant. Here $\gamma(\infty)$ denotes the damping coefficient in the corresponding bulk material. C_γ is a constant that is related to the Fermi velocity. Due to the simple geometry, the equivalent capacitance of series combination required to calculate the linear response, i.e., the optical absorption for the metallic film can be given by

$$\frac{1}{\bar{\epsilon}(\omega)} = \frac{1}{L}\int_0^L \frac{dz}{\epsilon(z,\omega)}. \tag{2.32}$$

The calculation of the local electric field $\mathbf{E}(z,\omega)$ can be given by the identity

$$\epsilon(z,\omega)\mathbf{E}(z,\omega) = \bar{\epsilon}(\omega)\mathbf{E}_0, \tag{2.33}$$

by virtue of the continuity of electric displacement.

The effective nonlinear response $\bar{\chi}(\omega)$ inside the graded film can be written as [70]

$$\bar{\chi}(\omega)\mathbf{E}_0^4 = \langle \chi(z,w)\left|\mathbf{E}_{\rm lin}(z)\right|^2 \mathbf{E}_{\rm lin}(z)^2\rangle, \tag{2.34}$$

where $\mathbf{E}_{\rm lin}(z)$ is the linear local electric field. Next the effective nonlinear response can be written as an integral over the layer, that is,

$$\bar{\chi}(\omega) = \frac{1}{L}\int_0^L dz\chi(z,\omega)\left|\frac{\bar{\epsilon}(\omega)}{\epsilon(z,w)}\right|^2\left[\frac{\bar{\epsilon}(\omega)}{\epsilon(z,\omega)}\right]^2. \tag{2.35}$$

In this thesis, $\chi(z,\omega)$ is set to be constant, in an attempt to emphasize the enhancement of the optical nonlinearity.

Chapter 3

Model and methods

In this thesis, the model is a two-component composite system as shown in Figure 1.1. Many particles with dielectric constant ϵ_1 and volume fraction f are randomly embedded in a homogeneous host medium with ϵ_2, in the presence of an external electric field E_0 along the z-axis. The dielectric constant of the suspended particle ϵ_1 is constant if the suspended particle is homogeneous. It is, however, a function of position $\epsilon_1(r)$ if the suspended particle is a functionally graded material (FGM).

The model is simple but the components maybe homogeneous or graded. Moreover, such composite system can be either isotropic or anisotropic. There exists many methods, both analytical and numerical, to calculate the effective dielectric properties of such system.

Rigorous calculation of the dielectric properties of a composite system is based on solving the Poisson's equation

$$\nabla \cdot [\epsilon(r) \nabla \Phi] = -\rho,$$

and obtaining the local potential, where $\epsilon(r)$ is a function of position r. In this thesis, the composite system has *no* free charge, that is, $\rho = 0$. Exact analytical solutions exist only for a handful of cases such as $\epsilon(r)$ being a constant, power-law and linear profile. The problem is analytically intractable for systems having an arbitrary profile of $\epsilon(r)$. Therefore, one has to rely on various approximations.

In this chapter, we provide the details of the approximations used for composite systems in this thesis.

3.1 Basic approximation methods

The effective dielectric constant ϵ_e is an important parameter which is used to investigated the dielectric properties of composite systems. In what follows, the well known basic approximation methods, i.e., Maxwell-Garnett theory (MGT), effective medium theory (EMT), Bergman-Milton spectral representation theory, and multiple images method are reviewed.

3.1.1 Maxwell-Garnett theory

The Maxwell-Garnett theory (MGT) [72, 73] is also known as the Clausius-Mossotti theory. It aims to predict the effective response of a composite without having to calculate the microscopic electric field. It can be used to study two-component composites such as our model, i.e., components with dielectric constant ϵ_1 and volume fraction f embedded in a medium with dielectric constant ϵ_2. Further, we approximate each particle as having a spherical shape. The calculation of the electric field and the induced dipole moment for a spherical particle have been given in Section 2.2.

We start by defining the molecular polarizability γ_{mol} of a single molecule:

$$\mathbf{p}_{mol} = \gamma_{mol}\epsilon_2\mathbf{E}_{mol}, \tag{3.1}$$

where $\mathbf{p}_{mol}$ is the induced dipole moment and $\mathbf{E}_{mol}$ is the polarizing electric field at the location of the molecule. For simplicity, we assume that there is no permanent polarization. We also assume that the polarizability is a scalar, since we restrict the treatment to uniform spherical inclusions.

The polarized field is produced by an external source and by the polarized molecules in the system except the one under study. We can image that we remove a small cavity of radius R around the molecule as shown in Figure 3.1. Now $\mathbf{E}_{mol}$ can be expressed as

$$\mathbf{E}_{mol} = \mathbf{E} - \mathbf{E}_p + \mathbf{E}_{near}, \tag{3.2}$$

where $\mathbf{E}$ is the macroscopic electric field given by Equation (2.14), $\mathbf{E}_{near}$ is the actual contribution of the molecules close to the given molecule, and $\mathbf{E}_p$ is the contribution from those molecules treated in an average continuum approximation described by the polarization $\mathbf{P}$. We assume that the structure of molecular compoiste is regular enough a cubical grid for example, or that they are randomly distributed. Lorentz showed that for atoms in a simple

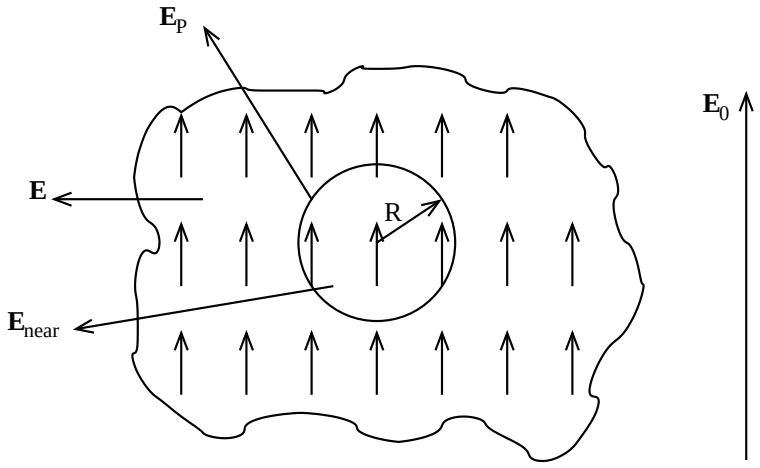

Figure 3.1: Electric fields for one molecule.

cubic lattice $\mathbf{E}_{near}$ vanishes at any lattice site [74], and it seems plausible that $\mathbf{E}_{near} = 0$ also for completely random situations.

If the volume V near the molecule is chosen to be sphere of radius R containing many molecules, the total dipole moment inside it is given by Equation (2.1), that is

$$\mathbf{p} = \frac{4\pi}{3} R^3 \mathbf{P}, \tag{3.3}$$

provided V is small enough such that $\mathbf{P}$ is essentially constant throughout the volume. The electric field in a uniformly polarized sphere is $-\mathbf{P}/(3\epsilon_2)$. Consequently, the polarized field is

$$\mathbf{E}_{mol} = \mathbf{E} + \frac{\mathbf{P}}{3\epsilon_2}. \tag{3.4}$$

The polarization vector $\mathbf{P}$ is defined in Equation (2.2) as

$$\mathbf{P} = N\langle \mathbf{p}_{mol} \rangle, \tag{3.5}$$

where $\langle \mathbf{p}_{mol} \rangle$ is the average dipole moment of the molecules. This dipole moment is proportional to the electric field acting on the molecule. According to the Equation (3.4),

$$\mathbf{P} = N\gamma_{mol}\epsilon_2 \left(\mathbf{E} + \frac{\mathbf{P}}{3\epsilon_2} \right). \tag{3.6}$$

On the other hand, $\mathbf{P} = (\epsilon_e - \epsilon_2)\mathbf{E}$, which results in the *Clausius-Mossotti equation*

$$\gamma_{mol} = \frac{3}{N}\frac{\epsilon_e - \epsilon_2}{\epsilon_e + 2\epsilon_2}, \tag{3.7}$$

where ϵ_e is the effective dielectric constant of the suspended particles.

The polarizability of a single sphere with radius a follows directly from the solution of the Laplace equation with a uniform background field $\mathbf{E_0}$. The induced dipole is given by Equation (2.17), i.e.,

$$\mathbf{p} = 4\pi a^3 \epsilon_2 \frac{\epsilon_1 - \epsilon_2}{\epsilon_1 + 2\epsilon_2}\mathbf{E}_0. \tag{3.8}$$

By using Equation (3.1), it is then clear that

$$\gamma_{mol} = 3V\frac{\epsilon_1 - \epsilon_2}{\epsilon_1 + 2\epsilon_2}, \tag{3.9}$$

where V is the volume of the sphere.

Homogenization of the composite means that the two expressions of polarizability are set to be equal. This yields the Maxwell-Garnett theory:

$$\frac{\epsilon_e - \epsilon_2}{\epsilon_e + 2\epsilon_2} = f\frac{\epsilon_1 - \epsilon_2}{\epsilon_1 + 2\epsilon_2}, \tag{3.10}$$

where $f = NV$ is the volume fraction of spheres ($0 \leq f \leq 1$). It is easy to check that this gives meaningful results for the special cases $\epsilon_1 = \epsilon_2$, $f = 0$, and $f = 1$.

The validity of this formula is best at low fractions, since its derivation is based on the analytical treatment of one sphere in an infinite space. Obviously, the MGT is an asymmetrical theory, that is, the physical properties of the composite can be changed if one exchanges the notations 1 and 2. The MGT can be extended straightforwardly to multi-component composites.

3.1.2 Effective medium theory

Effective medium theory was introduced by Bruggeman [75] (also known as the Bruggeman theory) and studied quantitatively by Landauer [76]. It is used to calculate the effective dielectric constant ϵ_e of a two-component composite system. The virtue of the method is that it is not limited to low concentrations of inhomogeneities or to weakly varying conductivities. Its predictions are usually physically sensible and offers insight into some

problems that are difficult to tract by other approaches. The suspended particles, instead of being embedded in their actual random environment, are immersed in a homogeneous effective medium of dielectric constant ϵ_e which will be determined self-consistently. Further, we assume the particle to be spherical. Then, the electric field inside the particles is uniform and given by (Equation (2.14))

$$\mathbf{E} = \frac{3\epsilon_e}{\epsilon_i + 2\epsilon_e}\mathbf{E}_0, \tag{3.11}$$

where $\epsilon_i = \epsilon_1$ or ϵ_2, and $\mathbf{E}_0$ is the applied electric field.

The self-consistency condition required by the EMA is that the average electric field within the particles shall be equal to E_0, or equivalently,

$$f\frac{3\epsilon_e}{\epsilon_1 + 2\epsilon_e}E_0 + (1-f)\frac{3\epsilon_e}{\epsilon_2 + 2\epsilon_e}E_0 = E_0. \tag{3.12}$$

The common factor E_0 may be divided out. Then this equation simplifies to the well-known form

$$f\frac{\epsilon_1 - \epsilon_e}{\epsilon_1 + 2\epsilon_e} = (1-f)\frac{\epsilon_2 - \epsilon_e}{\epsilon_2 + 2\epsilon_e}. \tag{3.13}$$

It is evident that the effective medium theory is a symmetrical theory, that is, the physical properties of the composite remain unchanged if one exchanges the notions 1 and 2. Extension to multi-component composites is straightforward.

3.1.3 Bergman-Milton spectral representation theory

The Bergman-Milton spectral representation theory is a rigorous mathematical formalism to express the effective dielectric constant of nongraded composite materials. Suppose the external electric field is along the z-axis. The problem is initiated by solving the differential equation [77]

$$\nabla \cdot \left[\left(1 - \frac{1}{s}\eta(\mathbf{r})\right)\nabla\phi(\mathbf{r})\right] = 0, \tag{3.14}$$

where $s = \epsilon_2/(\epsilon_2 - \epsilon_1)$ denotes the relevant material parameter and $\eta(\mathbf{r})$ is the characteristic function of the composite, having value 1 for r in the

embedding medium and zero otherwise. The electric potential $\phi(\mathbf{r})$ can be solved formally

$$\phi(\mathbf{r}) = z + \frac{1}{s}\int d\mathbf{r}'\eta(\mathbf{r}')\nabla' G_0(\mathbf{r}-\mathbf{r}')\cdot\nabla'\phi(\mathbf{r}'), \tag{3.15}$$

where $G_0(\mathbf{r}-\mathbf{r}') = |\mathbf{r}-\mathbf{r}'|/4\pi$ is the free space Green's function. We define an integral-differential operator as

$$\Lambda = \int d\mathbf{r}'\eta(\mathbf{r}')\nabla' G_0(\mathbf{r}-\mathbf{r}')\cdot\nabla', \tag{3.16}$$

and the corresponding inner product as

$$\langle\phi|\Phi\rangle = \int d\mathbf{r}\eta(\mathbf{r})\nabla\phi^*\cdot\nabla\Phi. \tag{3.17}$$

It is easy to show that Λ is a Hamiltonian operator. Let s_n and $\Phi_n(\mathbf{r})$ be the n-th eigenvalue and eigenfunction of Λ, Then we obtain the effective dielectric constant ϵ_e in the Bergman-Milton spectral representation theory as

$$\begin{aligned}
\epsilon_e &= -\frac{1}{V}\int dV\epsilon(\mathbf{r})E_z \\
&= \frac{1}{V}\int dV\epsilon_2\left[1-\frac{1}{s}\eta(\mathbf{r})\right]\frac{\partial\Phi}{\partial z} \\
&= \epsilon_2\left(1-\frac{1}{V}\sum_n\frac{|\langle\Phi_n|z\rangle|^2}{s-s_n}\right) \\
&= \epsilon_2\left(1-\sum_n\frac{F_n}{s-s_n}\right).
\end{aligned} \tag{3.18}$$

The parameters s_n and F_n satisfy the simple properties that $0 \le s_n \le 1$ and $\sum F_n = f$, where f is the volume fraction of the suspended particles. Equation (3.18) is just the effective dielectric constant of a two-component composite system in the Bergman-Milton spectral representation theory. Moreover, after introducing $F(s)$ as a function of s as

$$F(s) = \sum_n\frac{F_n}{s-s_n}, \tag{3.19}$$

we may readily obtain the spectral structure of the composite. In doing so, we may further represent $F(s)$ as

$$F(s) = \int_0^1 dx\frac{\nu(x)}{s-x}, \tag{3.20}$$

where the spectral function $\nu(x)$ is a crucial parameter which contains the information about the spectral structure. It is given by

$$\nu(x) = -\frac{1}{\pi}\mathrm{Im}F(x + i0^+). \tag{3.21}$$

The Bergman-Milton spectral representation theory offers the advantage of the separation of materials parameters (i.e., the permittivity or conductivity) from structural information (see Equation (3.18)), thus simplifying the analysis.

For example, MGT and EMT can be expressed by Bergman-Milton spectral representation theory. As a result, the $F(s)$ function and the spectral function for MGT respectively are

$$F(s) = \frac{f}{s-(1-f)/3}, \text{ and } \nu(x) = f\delta[x-(1-f)/3]. \tag{3.22}$$

As for EMT, we have

$$F(s) = \frac{1}{4s}\left(-1+3f+3s-3\sqrt{(s-x_1)(s-x_2)}\right), \tag{3.23}$$

where x_1 and x_2 are given by solving

$$(1-3f)2-6(1+f)x+9x^2 = 0, \tag{3.24}$$

and hence

$$x_1 = \frac{1}{3}\left(1+f-2\sqrt{2f(1-f)}\right), \text{ and } x_2 = \frac{1}{3}\left(1+f+2\sqrt{2f(1-f)}\right). \tag{3.25}$$

In this case, the spectral function should be

$$\nu(x) = \frac{3f-1}{2}\theta(3f-1) + \frac{3}{4\pi x}\sqrt{(x-x_1)(x_2-x)}, \tag{3.26}$$

as $x_1 < x < x_2$, and

$$\nu(x) = \frac{3p-1}{2}\theta(3p-1) \tag{3.27}$$

otherwise.

The Bergaman-Milton spectral representation theory can be extended to three-component composites by taking into account various approaches [78–80].

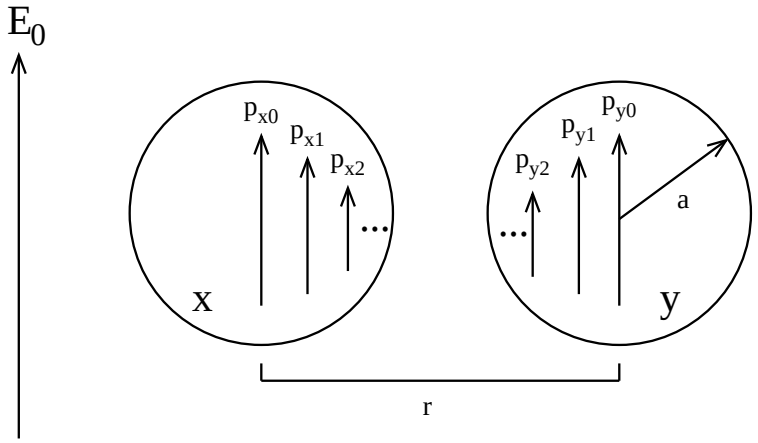

Figure 3.2: Schematic representation of the multiple images method. The total dipole moment is the sum of the induced dipole moments.

3.1.4 Multiple images method

This method calculates the multiple induced polarization between two colloidal particles x and y separated by a distance r. The particles are placed into a host medium with dielectric constant ϵ_2. Assume that the two particles are spheres with same radius a and that they are electrically neutral, and a constant electric field $\mathbf{E}_0 = E_0\hat{z}$ is applied to the spheres. Induced surface charge results in a dipole moment in each sphere given by $p_{x0} = 4\pi a^3\epsilon_2 bE_0$ and $p_{y0} = 4\pi a^3\epsilon_2 bE_0$, respectively. The dipole moment p_{x0} induces an image dipole p_{y1} in sphere y, while p_{y1} induces yet another image dipole in sphere x. Similarly, p_{y0} induces an image p_{x1} inside sphere x, leading to an infinite series of image dipoles. As a result, multiple images are formed as shown in Figure 3.2.

The total dipole moments of sphere x and y are given by [81]

$$\begin{aligned} p_L &= 4\pi a^3\epsilon_2 bE_0 \sum_{n=0}^{\infty}(2b)^n \left(\frac{\sinh\alpha}{\sinh(n+1)\alpha}\right)^3 \\ p_T &= 4\pi a^3\epsilon_2 bE_0 \sum_{n=0}^{\infty}(-b)^n \left(\frac{\sinh\alpha}{\sinh(n+1)\alpha}\right)^3, \end{aligned} \tag{3.28}$$

where L and T denote the longitudinal and transverse dipole moments, respectively, and α satisfies $\cosh\alpha = r/2a$. For two touching particles, the

effective dipole moment of a particle is given by

$$p^* = 4\pi a^3 \epsilon_2 b^* E_0, \tag{3.29}$$

where b^* is the effective dipole factor which is given by

$$b^* = \frac{1}{2} b \sum_{n=0}^{\infty} [(2b)^n + (-b)^n] \left(\frac{\sinh\alpha}{\sinh(n+1)\alpha} \right)^3. \tag{3.30}$$

Thus, we can use the final induced dipole factor to calculate the DEP force or electrorotation angular velocity.

3.2 Methods developed in this thesis

Over the past few years, there have been a number of attempts, both analytical and experimental, to study the responses of FGM to mechanical [82,83], thermal [84, 85], and electric [86, 87] loads, and for different microstructures in various systems. Numerous attempts have been made to treat the composite materials of homogeneous inclusions [23] as well as multishell inclusions [47, 88–90].

However, these established theories for homogeneous inclusions cannot be applied to graded composite materials. It is thus necessary to develop a new theory to study the effective properties of graded composite materials under externally applied fields. In this thesis, we developed a first-principles approach i.e., solving the Poisson's equation to calculate the effective responses of graded composite in which the dielectric constant $\epsilon(r)$ of one of the components has certain profiles, such as power-law and linear profile. Moreover, we developed a differential effective dipole approximation (DEDA) to calculate the effective dipole moment for isotropic graded composites, and anisotropic differential dipole approximation (ADEDA) for anisotropic graded particles. Furthermore, we developed a differential effective multipole moment approximation (DEMMA) as well an anisotropic differential effective multipole moment approximation (ADEMMA) to compute the multipole moment of a graded spherical particle in a nonuniform external field (produced by a point charge).

3.2.1 First-principles approach

In this section, we introduce the basic procedure of the first-principles approach. The suspended particle is a graded particle of dielectric constant

$\epsilon_1(r)$. We start from the dielectric response, and the constitutive relation of a graded spherical particle reads

$$\mathbf{D}_1 = \epsilon_1(r)\mathbf{E}_1. \tag{3.31}$$

The relation for the host medium is

$$\mathbf{D}_2 = \epsilon_2\mathbf{E}_2, \tag{3.32}$$

where ϵ_2 is the dielectric constant of the host medium, and it is a constant. The Maxwell's equations read

$$\nabla \cdot \mathbf{D} = 0, \tag{3.33}$$

and

$$\nabla \times \mathbf{E} = 0. \tag{3.34}$$

To this end, $\mathbf{E}$ is the gradient of a scalar function, the scalar potential, Φ:

$$\mathbf{E} = -\nabla\Phi. \tag{3.35}$$

Equation (3.33) and Equation (3.35) can be combined into one partial differential equation, the *Laplace Equation*:

$$\nabla \cdot [\epsilon(r)\nabla\Phi] = 0. \tag{3.36}$$

$\epsilon(r)$ is a dimensionless dielectric constant, $\epsilon(r) = \epsilon_1(r)/\epsilon_2$ in the particle, and $\epsilon(r) = 1$ in the host medium. Here we normalize the dielectric profile to the dielectric constant of the host medium ϵ_2 for convenience. Without loss of generality, we may also let the suspended graded particles be spheres with radius $a = 1$.

In spherical coordinates, the electric potential Φ satisfies

$$\begin{aligned} \frac{1}{r^2}\frac{\partial}{\partial r}\left(r^2\epsilon(r)\frac{\partial\Phi}{\partial r}\right) &+ \frac{1}{r^2\sin\theta}\frac{\partial}{\partial\theta}\left(\sin\theta\epsilon(r)\frac{\partial\Phi}{\partial r}\right) \\ &+ \frac{1}{r^2\sin^2\theta}\frac{\partial}{\partial\psi}\left(\epsilon(r)\frac{\partial\Phi}{\partial\psi}\right) = 0. \end{aligned} \tag{3.37}$$

We consider the applied electric field along the z-axis, thus Φ is independent of the angle φ. If we write $\Phi = R(r)\Theta(\theta)$, after a separation of variables, we obtain an ordinary differential equation for the radial function $R(r)$,

$$\frac{d}{dr}\left(r^2\frac{dR}{dr}\right) + \frac{r^2}{\epsilon(r)}\frac{d\epsilon(r)}{dr}\frac{dR}{dr} - n(n+1)R = 0, \tag{3.38}$$

where n is a integer.

The potential can be obtained by solving Equation (3.38) with boundary conditions, as follows:

$$\begin{aligned} \Phi_1(r,\theta)|_{r=1} &= \Phi_2(r,\theta)|_{r=1} \\ \epsilon_1(r)\left.\frac{\partial\Phi_1(r,\theta)}{\partial r}\right|_{r=1} &= \epsilon_2\left.\frac{\partial\Phi_2(r,\theta)}{\partial r}\right|_{r=1}, \end{aligned} \tag{3.39}$$

where $\Phi_1(r,\theta)$ and $\Phi_2(r,\theta)$ denote the potentials inside the suspended particles and the host medium, respectively. In the dilute limit, the dipole moment of the composite material can be derived. We take the average of the operator $\mathbf{D}-\epsilon_2\mathbf{E}$ in the whole volume of the composite material. That gives

$$\frac{1}{V}\int_V[\mathbf{D}-\epsilon_2\mathbf{E}]\mathrm{d}V = \bar{D}-\epsilon_2\bar{E}, \tag{3.40}$$

where V is the volume of the whole composite material. $\bar{A}$ denotes the average of the operator A in the composite material. The integrand vanishes in the host medium, and thus Equation (3.40) becomes

$$\frac{1}{V}\int_{\Omega_1}[\mathbf{D}-\epsilon_2\mathbf{E}]\mathrm{d}V = \bar{D}-\epsilon_2\bar{E}, \tag{3.41}$$

where Ω_1 is the volume occupied by the particle.

Now, we can define *Ohm's law* for the composite material:

$$\bar{D} = \epsilon_e\bar{E}, \tag{3.42}$$

where ϵ_e is the effective dielectric constant of the composite material. Thus

$$\frac{1}{V}\int_{\Omega_1}[(\epsilon_1(r)-\epsilon_2)\mathbf{E}]\mathrm{d}V = (\epsilon_e-\epsilon_2)\bar{E}. \tag{3.43}$$

Equation (3.43) gives the polarization of the composite material and it can be used to calculate the effective dielectric properties of the composite material at a low particle concentration. For example, the dipole factor can be calculated as

$$4\pi\epsilon_2E_0b = \int_{\Omega_1}[(\epsilon_1(r)-\epsilon_2)\mathbf{E}_1]\mathrm{d}V. \tag{3.44}$$

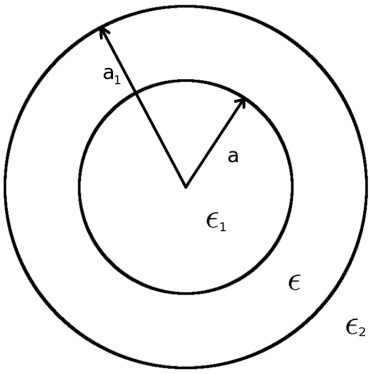

Figure 3.3: A schematic representation of one sphere with shell.

3.2.2 Differential effective dipole approximation

In this section, we give the details of DEDA for spherical particles of graded materials, and the corresponding result of effective dielectric response in the dilute limit. We start to use the two-component composite model for the homogeneous case, that is, the dielectric constants ϵ_1 and ϵ_2 are both constants. The suspended particle is sphere of radius a. The electric field strength is E_0. The induced dipole moment p is given by Equation (2.17), i.e.,

$$p = 4\pi a^3 \epsilon_2 b E_0, \tag{3.45}$$

where b is the dipole factor

$$b = \frac{\epsilon_1 - \epsilon_2}{\epsilon_1 + 2\epsilon_2}. \tag{3.46}$$

If we add a spherical shell of dielectric constant ϵ to make a coated sphere of overall radius a_1 as shown in Figure 3.3, then the induced dipole moment becomes

$$p_1 = 4\pi a_1^3 \epsilon_2 b_1 E_0, \tag{3.47}$$

where b_1 is the dipole factor of the coated sphere [12] given by

$$b_1 = \frac{(\epsilon - \epsilon_2) + (\epsilon_2 + 2\epsilon)x_1 y}{(\epsilon + 2\epsilon_2) + 2(\epsilon - 2\epsilon_2)x_1 y}, \tag{3.48}$$

where x_1 is given by

$$x_1 = \frac{\epsilon_1 - \epsilon}{\epsilon_1 + 2\epsilon}, \tag{3.49}$$

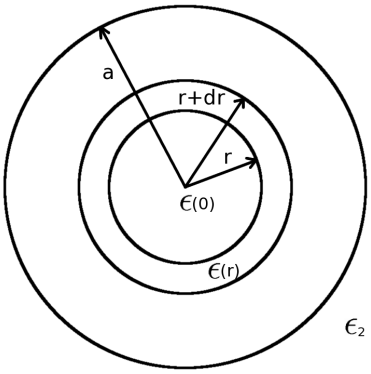

Figure 3.4: A schematic representation of one graded sphere with one shell.

and

$$y = \left(\frac{a}{a_1}\right)^3. \tag{3.50}$$

This can be extended to more shells of different dielectric constants at the expense of a more complicated expression [12]. It is easy to check that b_1 reduces to b when $\epsilon = \epsilon_1$. Thus, the dipole factor remains unchanged if one adds a spherical shell of the same dielectric constant.

Further, we consider an inhomogeneous sphere with dielectric profile $\epsilon(r)$ and radius a. To establish the differential effective dipole theory, we mimic the graded profile by a multi-shell construction, i.e., we build up the dielectric profile gradually by adding shells as shown in Figure 3.4. We start with an infinitesimal spherical core of dielectric constant $\epsilon(0)$ and keep on adding spherical shells of dielectric constant $\epsilon(r)$, until $r = a$ is reached. At radius r, we have an inhomogeneous sphere whose induced dipole moment is given by $p(r)$. Certainly $p(r)$ is proportional to E_0, but the exact expression is lacking. We further replace the inhomogeneous sphere by a homogeneous sphere of the same dipole moment and the graded profile is replaced by an effective dielectric constant $\bar{\epsilon}(r)$. Therefore,

$$p(r) = 4\pi r^3 \epsilon_2 b(r) E_0, \tag{3.51}$$

where

$$b(r) = \frac{\bar{\epsilon}(r) - \epsilon_2}{\bar{\epsilon}(r) + 2\epsilon_2}. \tag{3.52}$$

Next, we add a spherical shell of infinitesimal thickness dr, of dielectric constant $\epsilon(r)$. The dipole factor will change according to Equation (3.48). Of

course, the effective dielectric constant $\bar{\epsilon}(r)$, being related to $b(r)$, should also change. Let us write $b_1 = b + db$, and take the limit $dr \to 0$. We obtain a differential equation:

$$\frac{db}{dr} = -\frac{[(1+2b)\epsilon_2 - (1-b)\epsilon(r)]\,[(1+2b)\epsilon_2 + 2(1-b)\epsilon(r)]}{3r\epsilon_2\epsilon(r)}. \tag{3.53}$$

Thus the dipole factor of a graded spherical particle can be calculated by solving the above differential equation with a given graded profile $\epsilon(r)$. The nonlinear first-order differential equation can be solved, at least numerically, with the initial condition $b(r = 0)$.

3.2.3 Anisotropic differential effective dipole approximation

Due to gradation, anisotropic dielectric response occurs naturally. However, composite systems with local anisotropy are often macroscopically isotropic [91]. In this sense, the existing isotropic gradation models [92–94] for describing the isotropic graded particles are no longer valid, and anisotropic differential effective dipole approximation (ADEDA) is developed.

ADEDA is a numerical method which is put forth for the analysis of the properties of arbitrarily graded anisotropic particles. Its derivation is based on a two-component composite system. The host medium is homogeneous. The graded spherical particle has a tangential permittivity in the plane orthogonal to the radial vector of the sphere $[\epsilon_{\theta\theta}(r) = \epsilon_{\phi\phi}(r)]$, and radial permittivity $\epsilon_{rr}(r)$. In view of the spherical symmetry, the dielectric anisotropy of the graded sphere can be expressed by means of the permittivity tensor $\overleftrightarrow{\epsilon}_c$ [95]:

$$\overleftrightarrow{\epsilon}_c(r) = \begin{bmatrix} \epsilon_{rr}(r) & 0 & 0 \\ 0 & \epsilon_{\theta\theta}(r) & 0 \\ 0 & 0 & \epsilon_{\phi\phi}(r) \end{bmatrix}. \tag{3.54}$$

Next, we follow the same procedure as in the derivation of DEDA. Now permittivity has two components $\epsilon_{\theta\theta}(r)$ and $\epsilon_{rr}(r)$. The dipole factor should change according to the dipole factor of one shell anisotropic composite inclusion [95], that is

$$b_1(r) = \frac{\dfrac{\epsilon_{rr}(r)\delta_+ - \epsilon_2}{\epsilon_{rr}(r)\delta_+ - \bar{\epsilon}(r)} - \dfrac{\epsilon_{rr}(r)\delta_- - \epsilon_2}{\epsilon_{rr}(r)\delta_- - \bar{\epsilon}(r)}\rho}{\dfrac{\epsilon_{rr}(r)\delta_+ + 2\epsilon_2}{\epsilon_{rr}(r)\delta_+ - \bar{\epsilon}(r)} - \dfrac{\epsilon_{rr}(r)\delta_- + 2\epsilon_2}{\epsilon_{rr}(r)\delta_- - \bar{\epsilon}(r)}\rho}, \tag{3.55}$$

where

$$\begin{aligned}
\delta_+ &= \frac{1}{2}\left[-1+\sqrt{1+\frac{8\epsilon_{\theta\theta}(r)}{\epsilon_{rr}}}\right] \\
\delta_- &= \frac{1}{2}\left[-1-\sqrt{1+\frac{8\epsilon_{\theta\theta}(r)}{\epsilon_{rr}}}\right] \\
\rho &= \left(\frac{r}{r+dr}\right)^{\delta_+-\delta_-}.
\end{aligned} \tag{3.56}$$

Let us write further $b_1(r) = b(r) + \mathrm{d}b$, and take the limit $\mathrm{d}r \to 0$. Then the desired correction $\mathrm{d}b$ is infinitesimal. Thus, one obtains a differential equation:

$$\begin{aligned}
\frac{\mathrm{d}b(r)}{\mathrm{d}r} &= -\frac{1}{3r\epsilon_{rr}(r)\epsilon_2}\left[(1+2b(r))\epsilon_2-(1-b(r))\delta_+\epsilon_{rr}(r)\right] \\
&\quad \left[(1+2b(r))\epsilon_2-(1-b(r))\delta_-\right],
\end{aligned} \tag{3.57}$$

where $0 < r < a$. This equation reduces to (Equation (3.53)) if $\delta_+ = 1$, $\delta_- = -2$ and $\rho = 3$, i.e., $\epsilon_{rr}(r) = \epsilon_{\theta\theta}(r)$, ADEDA reduces to the isotropic case — DEDA.

Therefore, the dipole factor of a graded anisotropic spherical particle can be calculated by solving the first-order differential equation (Equation (3.57)). This differential equation can be integrated, at least numerically, if we are given the gradation profiles $\epsilon_{\theta\theta}(r)$ and $\epsilon_{rr}(r)$, and the initial condition $b(0)$.

3.2.4 Differential effective multipole moment approximation

The problem of a dielectric sphere interacting with a point charge is more general than the uniform applied electric field, because the nonuniform field of the point charge induces all the linear multipolar moments – that is, the dipole, quadrupole, octopole, etc. Differential effective multipole moment approximation is developed to compute the multipole moment of a graded spherical particle in a nonuniform external electric field produced by a point charge.

We consider a graded spherical particle of radius a subjected to a nonuniform electric field of a point charge Q placed on the z-axis as shown in Figure 3.5.

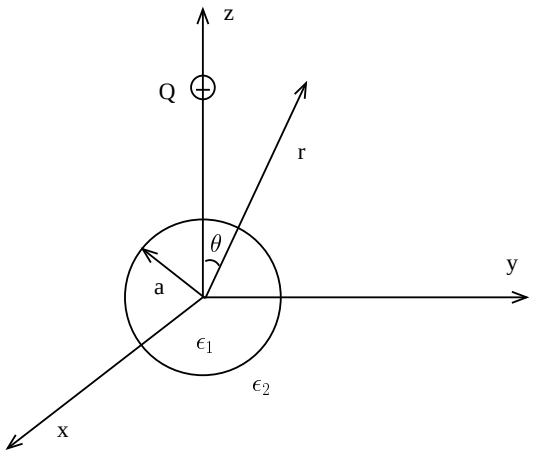

Figure 3.5: A schematic representation of particle in electric field produced by point charge.

The derivation of DEMMA is similar to that of DEDA, only the dipole factor b is replaced by multipole factor $H_l(r)$ [96]

$$H_l(r) = \frac{l(\bar{\epsilon}(r) - \epsilon_2)}{l(\bar{\epsilon}(r) + \epsilon_2) + \epsilon_2}. \tag{3.58}$$

It is easy to see that for $l = 1$,

$$H_1(r) = \frac{\bar{\epsilon}(r) - \epsilon_2}{\bar{\epsilon}(r) + 2\epsilon_2} \tag{3.59}$$

is the dipole factor $b(r)$ (Equation (3.52)).

Next, we add a spherical shell of infinitesimal thickness dr of permittivity $\epsilon_1(r)$. The resulting multipole factor H_l' will change according to [97]

$$H_l{}' = \frac{[l'\epsilon(r) + l\bar{\epsilon}(r)]\,[l\epsilon(r) - l\epsilon_2] - \rho\,[l\epsilon(r) - l\bar{\epsilon}(r)]\,[l'\epsilon(r) + l\epsilon_2]}{[l'\epsilon(r) + l\bar{\epsilon}(r)]\,[l\epsilon(r) + l'\epsilon_2] - \rho ll'\,[\epsilon(r) - \bar{\epsilon}(r)]\,[\epsilon(r) - \epsilon_2]}, \tag{3.60}$$

with $l' = l + 1$ and $\rho = [r/(r + dr)]^{2l+1}$.

Of course, the equivalent permittivity $\bar{\epsilon}(r)$, being related to $H_l(r)$, should also change. Let us write $H_l' = H_l + dH_l$, and take the limit $dr \to 0$. We obtain a differential equation:

$$\begin{aligned} \frac{dH_l(r)}{dr} &= -\frac{1}{(2l+1)r\epsilon_2\epsilon(r)} \\ &\quad \times [(l + (1+l)H_l(r))\epsilon_2 - l(1 - H_l(r))\epsilon(r)] \\ &\quad \times [(l + (1+l)H_l(r))\epsilon_2 + (l+1)(1 - H_l(r))\epsilon(r)]\,. \end{aligned} \tag{3.61}$$

It is easy to notice that Equation (3.61) reduces to Equation (3.53) as $l = 1$.

When we substitute Equation (3.58) into Equation (3.61), we obtain a differential equation for the equivalent dielectric constant $\bar{\epsilon}(r)$

$$\frac{d\bar{\epsilon}(r)}{dr} = \frac{[\epsilon(r) - \bar{\epsilon}(r)][(l+1)\epsilon(r) + l\bar{\epsilon}(r)]}{r\epsilon(r)}. \tag{3.62}$$

Setting $l = 1$ in the above equation is a special case of the Tartar formula derived for assemblies of spheres with varying radial and tangential conductivities [98].

3.2.5 Anisotropic differential effective multipole moment approximation

The differential effective multipole moment approximation can be extended to the anisotropic case, that is, the suspended spherical particle has a tangential permittivity in the plane orthogonal to the radial vector of the sphere $[\epsilon_{\theta\theta}(r) = \epsilon_{\phi\phi}(r)]$, and radial permittivity $\epsilon_{rr}(r)$. In view of the spherical symmetry, the dielectric anisotropy of the graded sphere can be expressed by means of the permittivity tensor $\overleftrightarrow{\epsilon}_c$ [95] given by Equation (3.54). The derivation of anisotropic differential effective multipole moment approximation (ADEMMA), which is similar to DEMMA, is a numerical method for the analysis of the electric properties of anisotropic graded particles with arbitrary gradation profiles. Similarly, we may regard the gradation profile as a multishell construction. Let us start with an infinitesimal isotropic spherical core with permittivity $\epsilon(0^+)$, and keep on adding shells with both tangential and normal permittivity profiles $\epsilon_{\theta\theta}(r)$ and $\epsilon_{rr}(r)$ until $r \to a$ is reached. At radius r, we have an inhomogeneous particle with effective permittivity $\bar{\epsilon}(r)$, which has the multipole factor

$$H_l(r) = \frac{l(\bar{\epsilon}(r) - \epsilon_2)}{l(\bar{\epsilon}(r) + \epsilon_2) + \epsilon_2}. \tag{3.63}$$

As before, we add a shell with infinitesimal thickness dr with permittivities $\epsilon_{\theta\theta}(r)$ and $\epsilon_{rr}(r)$. The multipole factor H_l' should change according to the multipole factor of a single-coated particle [99]

$$H_l' = \frac{\dfrac{\epsilon_{rr}(r)u_+ - l\epsilon_2}{\epsilon_{rr}(r)u_+ - l\bar{\epsilon}(r)} - \rho_l \dfrac{\epsilon_{rr}(r)u_- - l\epsilon_2}{\epsilon_{rr}(r)u_- - l\bar{\epsilon}(r)}}{\dfrac{\epsilon_{rr}(r)u_+ + l'\epsilon_2}{\epsilon_{rr}(r)u_+ - l\bar{\epsilon}(r)} - \rho_l \dfrac{\epsilon_{rr}(r)u_- + l'\epsilon_2}{\epsilon_{rr}(r)u_- - l\bar{\epsilon}(r)}}, \tag{3.64}$$

with $l' = l + 1$ and

$$\begin{aligned} u_{\pm} &= [-1 \pm \sqrt{1 + 4l(l+1)\epsilon_{\theta\theta}(r)/\epsilon_{rr}(r)}]/2 \\ \rho_l &= [r/(r+dr)]^{u_+ - u_-}. \end{aligned} \tag{3.65}$$

Let us write further $H_l' = H_l + dH_l$, and take the limit $dr \to 0$. We obtain a differential equation

$$\begin{aligned} \frac{dH_l(r)}{dr} &= -\frac{1}{(2l+1)r\epsilon_2\epsilon(r)} \\ &\quad \times [(l + l'H_l(r))\epsilon_2 - (1 - H_l(r))u_+\epsilon_{rr}(r)] \\ &\quad \times [(l + l'H_l(r))\epsilon_2 - (1 - H_l(r))u_-\epsilon_{rr}(r)]\,. \end{aligned} \tag{3.66}$$

This equation is the general form of the differential effective approximation. It reduces to DEMMA when $\epsilon_{rr} = \epsilon_{\theta\theta}$, and further reduces to DEDA when $l = 1$. Thus, the multipole factor of an anisotropic graded spherical particle $H_l(r = a)$ can be calculated by solving the nonlinear first-order differential equation (Equation (3.66)) which can be integrated, at least numerically, if the profiles $\epsilon_{\theta\theta}(r)$, $\epsilon_{rr}(r)$ and the initial condition $H_l(r = 0)$ are given. The substitution of Equation (3.63) into Equation (3.66) yields the differential equation for the equivalent permittivity

$$\frac{d\bar{\epsilon}(r)}{dr} = \frac{(1+l)\epsilon_{\theta\theta}(r)\epsilon_{rr}(r) - \epsilon_{rr}(r)\bar{\epsilon}(r) - l\bar{\epsilon}(r)^2}{r\epsilon_{rr}(r)}. \tag{3.67}$$

Equations (3.66) and (3.67) can respectively be reducee to Equations (3.61) and (3.62), as long as $\epsilon_{\theta\theta}(r) = \epsilon_{rr}(r)$. The substitution of $l = 1$ into Equation (3.67) yields the Tartar formula [98].

Chapter 4

Overview of results

This thesis focuses on thoretical study of dielectric properties of colloidal particles. It consists of two parts. In the first part the attention is on the dielectrophoresis (DEP) spertrum of two touching spherical homogeneous colloidal particles by considering the effect of multiple images. This reserach is covered by Publication I. Publications II-VII, the second part of the thesis, address the effective dielectric properties of functionally graded materials using various methods. In them, the graded profile ϵ can be either isotropic or anisotropic. For certain profiles, the dipole factor can be obtained analytically; for the arbitrary profiles, it is computed by developed approximate methods. It is notable, that the approximate results agree well with the analytical results.

Publication I was motivated by the results of Ref. [100], which demonstrates that the multiple images method agrees with the multipole expansion method and the multiple images method reflects, although not exactly, some characteristics of the third order multipole expansion method, i.e., an octopole effect. In this work, by employing the spectral representation theory [77], we derived an analytic expression for the DEP force and hence determined the DEP spectrum as well as crossover frequency with the influence of interactive polarization. We investigated two cases: (1) the longitudinal field case where the applied field is parallel to the line joining the centers of the two particles, and (2) the transverse field case where the applied field is perpendicular to the line joining the centers of the two particles. We also compared the DEP spectra for an isolated particle and for two touching particles.

The results show that the effect of multiple images play an important role in the DEP spectrum in the low frequency region. The effect increases (decreases) the induced-dipole moment of the individual particles in the longitu-

dinal (transverse) geometry, and hence the DEP force can be enhanced (reduced) significantly for the longitudinal (transverse) field case. The crossover frequency in the longitudinal (transverse) case moves to the lower (higher) frequencies in the case where the particles are in contact. This is due to the effect of multiple images.

Publication II presents a first-principles approach and an anisotropic differential effective dipole approximation (ADEDA), respectively, for the calculation of the dipole moment of anisotropic graded particles. This work is an extension of Ref. [93] which calculates the dipole moment of isotropic graded particles by combining a first-principles approach with the differential effective dipole approximation (DEDA). The results of this studies found that there is an exact solution when the gradation profile is a linear radial function. We evaluate the ADEDA by considering a linear gradation profile. The numerical integration has been done by the fourth-order Runge-Kutta algorithm with step size 0.01. The agreement is excellent. Thus, ADEDA is a very good approximation for anisotropic graded spherical particles.

The fact that ADEDA shows very good agreement with the first-principles approach is encouraging as ADEDA allows us to treat arbitrary gradation profiles in realistic problems, such as optical properties of anisotropic graded materials, and electrokinetic behaviors of biological cells.

Publication III addresses the optical nonlinear properties of graded materials. In contrast to bulk materials, the corresponding thin films often prossesses inhomogeneous optical properties [14, 101]. It is also known that graded materials [26, 98] have quite different physical properties from homogeneous materials. In addition, graded thin films may have better dielectric properties than single-layer films [102]. Moreover, there is a wide range of applications for nonlinear optical materials with large nonlinear susceptibility or optimal figure of merit (FOM). However, the surface plasmon resonant nonlinear enhancement often occurs concomitantly with a strong absorption, and unfortunately this behavior renders the FOM of the resonant enhancement peak too small to be useful. To circumvent this problem, we considered a graded metal-dielectric composite film, in which the dielectric component is introduced as spherical particles embedded in a metallic component.

When the layer dielectric profile of form $p(z) = az^m$ is taken into account, a broad resonant plasmon band is always observed. In other words, the broad band is caused by the effect of the positional dependence of the dielectric or metal. Also, we found that increasing a causes the resonant band not only to be enhanced, but also to be red-shifted (e.g., located at a lower frequency region). The present results do not depend crucially on the particular form of

the layer dielectric profile $p(z)$. The only requirement is that there must be a composition-dependent layer to yield a broad plasmon band for the graded film. It should be noted that the optical response of a graded structure depends on polarization of the incident light, because the incident optical field can always be resolved into two polarizations. However, a large nonlinear enhancement occurs only when the electric field is parallel to the direction of the gradient [103], and the other polarization does not produce nonlinear enhancement [103].

Publication IV was motivated by the study of the optical absorption spectrum of a graded metallic film [104]. In this work, a broad surface plasmon absorption band was observed in addition to a strong Drude absorption peak at zero frequency. Such a broad absorption band has been shown to be responsible for the enhanced nonlinear optical response as well as an attractive figure of merit (the degree of optical absorption). Yuen *et al.* [105] pointed out that such an absorption spectrum, being related to the imaginary part of the effective dielectric constant, should be also reflected in the Bergman-Milton spectral representation of the effective dielectric constant [106–108]. This work on grade film is an example of a more general work on graded composite in three dimensions. One of the main purposes of this work is to help identify the physical origin of the broad absorption band. Contrary to the case of homogeneous materials, the characteristic function of a graded composite is a continuous function due to the continuous variation of the dielectric function within the constituent component. Moreover, we apply our theory to a special case of graded composites, namely multilayer materials. From a practical point of view, they are more convenient to fabricate than graded materials [15] and, in addition are more reality available for designing multilayer coatings [16, 17].

The results of Publication IV present a graded composite film and a sphere by means of the Bergman-Milton spectral representation. It was shown that the spectral density function can be obtained analytically for a graded system. However, unlike in the case of homogeneous constituent components, the characteristic function is a continuous function due to the presence of gradation. The derivation, as well as some salient properties, including the sum rules, the definition of the inner product, the definition of the integral-differential operators, and the range of spectral parameters, change because of the continuous variation of the dielectric profile within the constituent components. This work also studied multilayer composites and calculated the spectral density function versus the number of layers in order to explicitly demonstrate that the broad continuous spectrum arises from the accumulation of poles when the number of layers tends to infinity. This finding

agrees with the experimentally observed broad surface-plasmon absorption band associated with the optical properties of graded composites [109].

Publication V extends the first-principles calculations of dielectric responses of graded particles in uniform electric field. In this case, the particles are sufficiently far apart so that it is possible to neglect contributions form higher-order multipoles. As the separation of the particles decreases, the local field becomes extremely inhomogeneous especially near the surface of the particles. In this work, we studied the multipole polarizability of a graded spherical particle in a nonuniform field due to a point charge. The electrostatic boundary-value problem of a graded spherical particle was solved to obtain exact analytic results for a power-law profile. For arbitrary profiles, we developed a differential effective multipole moment approximation (DEMMA) to compute the multipole moment of a graded spherical particle to capture the multipole response in a nonuniform field. The results of the first-principles approach and that of DEMMA agree with each other. However, DEMMA is a numerical method which can be applied to an arbitrary profile.

Moreover, DEMMA is extended to anisotropic differential effective multipole moment approximation (ADEMMA), which is used to calculated the dielectric responses of anisotropic graded materials, and it is applicable to a general case.

Publication VI was motivated by Publication III and IV. Publication III investigates the enhancement of optical nonlinearity in compositionally graded metal-dielectric films in which the fraction of metal component varies perpendicular to the film. Publication IV found that there is always a broad continuous function in the spectral density function in graded composite, but simple poles in multilayer composite, and the number of the poles depends on the number of layers. In this work, the results show that the optical absorption spectrum and the enhancement of optical nonlinearity consist mainly of sharp peaks. However the strong optical absorption and the large fluctuation of the nonlinear optical enhancement near these sharp peaks render the FOM too small for industrial applications. When the number of layers becomes large, the sharp peaks accumulate to a broad band while the fluctuations are reduced significantly. In this limit, the broad continuous absorption band emerges, and a large FOM persists. To sum up, as the number of layers inside the metallic films increases, a gradual transition from sharp peaks to a broad continuous band emerges until the graded film results are recovere. This agrees with the results in Publication IV.

The work in Publication VII is a first-principles approach. It gives the analytical solution of local potentials of graded particles in terms of hypergeometric

functions when the dielectric constant of suspended particles assume a profile of the form $\epsilon_1(r) = A + cr^k$, where r is the radius of the suspended spherical particle, and A, c and k are constants. Our analytical results are useful for analyzing the bulk AC response of graded colloidal suspensions and for the control of the dielectric response of functionally graded materials having complex dielectric graded profile.

Chapter 5

Summary

In this thesis dielectric properties of colloidal suspension were studies theoretically. It consists of the study of dielectrophoresis spectrum of two touching spherical particles in suspensions and the study of effective dipole factor of functionally graded materials in suspensions. We adopted analytical methods and various approximate methods. The results obtained from this various methods show excellent agreement.

We attempted a theoretical study of dielectrophoresis (DEP) of two approaching spherical particles by considering the effect of mutual polarization. When two particles approach and finally touch, the mutual polarization interaction between them leads to a change in the dipole moment of individual particles and hence the DEP spectrum, as compared to that of the well-separated particles. This effect of mutual polarization is studied via the multiple image methods as shown in Figure 3.2. From the results, we found that the effect of mutual polarization can change the characteristic frequency as well as the magnitude of dielectrophoresis spectrum. In view of the results of a two-particle system under consideration in this work, an extension to higher concentrations is necessary. In doing so, we could resort to an effective medium theory to include many-body (local-field) effects [110]. This theory can be applied to investigate the dependence of DEP spectra on gradation (inhomogeneity) [92, 93] inside colloidal particles or biological cells. We should point out that the multiple images method is approximate method [111] but this approximation is quite good [81], and the computation is cheap. In addition, charge, temperature and Brownian motion are not included in our analysis, these factors are always present in experiments. Work is in progress to address these questions. And some of them have been solved in literature [112–114].

In this thesis, we applied First-principles approach which is an analytical method. It only gives solutions for certain graded profile ϵ, such as power-law, linear and exponential profiles, and the solving procedure is complicated. Note that having one exact solution yields much insight and such solution could be useful as benchmark. The Begman-Milton spectral representation is a rigorous mathematical formalism and was originally developed for calculating the effective dielectric constant and other response functions of two-component composites. However, in the original representation both of the two components concerned are assumed to be homogeneous. In this thesis, we extended it to graded composite materials. We also studied multilayer composite and calculated the spectral density function versus the number of layers in order to explicitly demonstrate that the broad continuous spectrum arises from the accumulation of poles when the number of layers tends to infinity. The spectral representation approach separates the material parameter from the structure parameter, then we can investigate the effect of material parameter and structure parameter, respectively. In this thesis, we studied the effect the structure parameter, and the spectral representation visualize the graded structure.

We developed several approximate methods in this thesis. Anisotropic differential effective dipole approximation (ADEDA) is an extension of differential effective dipole approximation (DEDA) to calculate the effective dipole factor of graded materials. Its results show excellent agreement with the results from first-principles approach. Colloidal suspensions and many kinds of cells have non-spherical shapes, e.g., red blood cells are oblate spheroids. The derivation of DEDA for non-spherical particles had been done [92], hence similar work for ADEDA is also possible to be extended. It would be also interesting to compare this theory to experimental results. Further work could be extended to discuss the dielectrophoresis spectrum of a pair of graded anisotropic particles by taking into account the effect of multiple images and to investigate high concentration suspensions by discussing the many-body (local field) effects [115]. A generalization which includes both of these effects is of particular interest.

We also developed a differential effective multipole moment approximation (DEMMA) to compute the multipole factor of a graded spherical particles in a nonuniform electric field due to a point charge. We compared the DEMMA results with the exact results for the power-law dielectric profile and the agreement is excellent. As the multipole response is sensitive to the graded profile of the particles as well as to the structure of the nonuniform field source, there is a potential application to AC electriokinetics of graded colloidal particles [116]. The similar approach can be applied to electrorheolog-

ical fluids [117,118] because the particles in electrorheological fluids can have very dense structures locally. The local electric fields are extremely inhomogeneous near the particles so that multipole effects can play an important role. In this regards, DEMMA could be extended to study the interparticle force between graded particles [81] in electrorheological fluids. In the other topics, based on the calculation of DEMMA, the similar calculation of the multipole response of a graded metallic sphere in the nonuniform field of an oscillating point dipole at optical frequency could be attempted. When the oscillating source is placed close enough to the graded metallic sphere, higher-order multipole response can be excited. The approach may also be applied to the electroencephalogram of the human brain by regarding the brain as a graded anisotropic conducting sphere. For the anisotropic case, anisotropic DEMMA can be applied.

Nonlinear optical materials with a large value of the third-order nonlinear susceptibility are in great need in industrial applications. In this thesis, we investigate the nonlinear optical enhancement in graded metallic materials and in multilayer metallic films. Our preliminary results show that the final representation and the definition of the spectral density function remain the same as the Bergman-Milton representation [77]. Moreover, the separation of the material parameter from the structure innformation still holds. Also, it is interesting to extend the present consideration to composites in which graded spherical particles are embedded in a host medium to account for mutual interationcs among graded particles. Similar considerations can be extended to other nonlinear optical properties such as the second-harmonic generation [119].

Bibliography

[1] D. F. Evans and H. Wennerström, *The Colloidal Domain: Where Physics, Chemistry, Biology and Technology Meet* (Wiley-VCH, New York, 1999).

[2] P.-G. de Gennes, J. Badoz, and translated by Axel Reisinger, *Fragile Objects: Soft Matter, Hard Science and the Thrill of Discovery* (Springer-Verlag New York, Inc, New York, 1996).

[3] A. P. Philipse, in *Fundamentals of Interface and Colloid Science*, edited by J. Lyklema (Elsevier, Amsterdam, 2005), Vol. IV, p. 2.1.

[4] E. Hatschek, *The Foundations of Colloid Chemistry: a Selection of Early Papers Bearing on the Subject* (E. Benn Ltd., London, 1925).

[5] Graham, Phi. Trans. Roy. Soc. **151**, 183 (1861).

[6] O. D. Velev, A. M. Lenhoff, and E. W. Kaler, Science **287**, 2240 (2000).

[7] A. Vrij and R. Tuinier, in *Structure of Concentrated Colloidal Dispersions*, edited by J. Lyklema (Elsevier, Amsterdam, 2005), Vol. IV, p. 5.1.

[8] D. L. Fedlheim and C. A. Foss, *Metal Nanoparticles: Synthesis Characterization and Applications* (Marcel Dekker, New York, 2002).

[9] L. M. Liz-Marzan, Materials Today **7**, 26 (2004).

[10] Y. Miyamoto *et al.*, *Functionally Graded Materials: Design, Processing and Applications* (Kluwer Academic Publishers, Massachusetts, USA, 1999).

[11] in *Proceedings of the First International Symposium on Functionally Gradient Materials*, edited by M. Yamanouchi, M. Koizumi, T. Hirai, and I. Shiota (Functionally Gradient Materials Forum, Sendai, Japan, 1990).

[12] in *Ceramic Transaction: Functionally Graded Materials*, edited by T. H. J. B. Holt, M. Koizumi and Z. A. Munir (The American Ceramic Society, Westerville, 1993), Vol. 34.

[13] in *Proceedings of the First International Symposium on Functionally Graded Materials*, edited by B. Ilschner and N. Cherradi (Presses Polytechniquies et Universititaires Romands, Lausanne, 1994).

[14] D. R. Kammler *et al.*, J. Appl. Phys. **50**, 5797 (2001).

[15] M. P. Hobson and J. E. Baldwin, Appl. Opt. **43**, 2651 (2004).

[16] S. Martin, J. Rivory, and M. Schoenauer, Appl. Opt. **34**, 2247 (1998).

[17] P. G. Verly, Appl. Opt. **37**, 7327 (1998).

[18] R. J. Botsco, R. W. Cribbs, R. J. King, and R. C. McMaster, *Microwave Methods and Applications in Nondestructive Testing, in Nondestructive Testing Handbook*, R. C. McMaster and Pual McIntire (Eds), Second Edition, Vol. 4 (American Society Nondestructive Testing, 1986).

[19] B. K. P. Scaife, *Principles of Dielectrics* (Oxford Science Publications, Oxford, 1998).

[20] H. Frohlich, *Theory of Dielectrics: Permittivity and Dielectric Loss* (Oxford Science Publications, Oxford, 1958).

[21] C. J. F. Bottcher, *Theory of Electric Polarization* (Elsevier Publishing Company, Amsterdam, 1952).

[22] *Basics of measuring the dielectric properties of materials*, Hewlett Packard literature number 5091-3300E, 1992, application Note 1217-1.

[23] J. D. Jackson, *Classical Electrodynamics* (John Wiley & Sons, Inc., New York, 1975).

[24] A. Tiselius, Trans. Faraday Soc. **33**, 524 (1937).

[25] H. A. Pohl, *Dielectrophoresis* (Cambridge University Press, Cambridge, 1978).

[26] T. B. Jones, *Electromechanics of Particles* (Cambridge University Press, Cambridge, 1995).

[27] U. Zimmermann and G. A. Neil, *Electromanipulation of Cells* (CRC Press, Boca Raton, FL, 1995).

[28] E. Hatschek and P. C. L. Thorne, Proc. R. Soc. London **103**, 276 (1923).

[29] H. A. Pohl, J. Appl. Phys. **22**, 869 (1951).

[30] P. R. C. Gascoyne, R. Pething, J. P. H. Burt, and F. F. Becker, Biochim. Biophys. Acta **1149**, 119 (1993).

[31] K. V. I. S. Kaller and T. B. Jones, Biophys. J. **57**, 173 (1990).

[32] H. A. Pohl and I. Hawk, Science **152**, 647 (1996).

[33] Y. Huang, R. Hozel, R. Pething, and X. B. Wang, Phys. Med. Biol. **37**, 1499 (1992).

[34] M. P. Hughes and H. Morgan, Biotechnol. Prog. **245**, 15 (1999).

[35] U. Zimmermann, J. Vienken, and P. Scheurich, Biophys. Struct. Mech. **6**, 86 (1980).

[36] U. Zimmermann, Biochim. Biophys. Acta **694**, 227 (1992).

[37] I. G. Abidor and A. E. Sowers, Biophys. J. **61**, 1557 (1992).

[38] G. H. Markx and R. Pething, Biotechnol. Bioeng. **45**, 337 (1994).

[39] P. R. C. Gascoyne *et al.*, Meas. Sci. Techonol. **3**, 439 (1992).

[40] J. Rousselet, L. Salome, A. Ajdari, and J. Prost, Nature **370**, 446 (1994).

[41] T. B. Jones and G. W. Bliss, J. Appl. Phys. **48**, 1412 (1977).

[42] I. J. Lin and T. B. Jones, J. Electrostatics **15**, 53 (1984).

[43] X. B. Wang, Y. Huang, F. F. Becker, and P. Gascoyne, J. Phys. D: Appl. Phys. **27**, 1571 (1994).

[44] T. B. Jones and M. Washizu, J. Electrostatics **37**, 121 (1996).

[45] A. A. Teixeira-Pinto, L. L. Nejelski, J. L. Culter, and J. H. Heller, J. Exp. Cell Res. **20**, 548 (1960).

[46] C. Holzapfel, J. Vienken, and U. Zimmermann, J. Membrane Biol. **67**, 13 (1982).

[47] W. M. Arnold and U. Zimmermann, Z. Matureforsch. **37c**, 908 (1982).

[48] W. M. Arnold and U. Zimmermann, J. Electrostatics **21**, 151 (1988).

[49] X. F. Zhou, G. H. Markx, R. Pething, and I. Eastwood, Biochim. Biophys. Acta **1245**, 85 (1995).

[50] J. S. Batchelder, Rev. Sci. Instrum. **54**, 300 (1983).

[51] S. Masuda, M. Washizu, and M. Iwadare, IEEE Trans. Ind. Appl. **23**, 474 (1987).

[52] S. Masuda, M. Washizu, and I. Kawabata, IEEE Trans. Ind. Appl. **24**, 217 (1988).

[53] G. Fuhr *et al.*, Stud. Biophys. **140**, 79 (1991).

[54] Y. Huang, X. B. Wang, J. Tame, and R. Pething, J. Phys. D: Appl. Phys. **26**, 312 (1993).

[55] Y. Huang and R. Pething, Meas. Sci. Technol. **2**, 1142 (1991).

[56] P. Drazin and R. Johnson, *Solitons: An Introduction* (Cambridge University Press, Cambridge, UK, 1989).

[57] R. W. Boyd, *Nonlinear Optics* (Academic, New York, 1992).

[58] M. Nielsen and I. Chuang, *Quantum Computation and Quantum Information* (Cambridge University Press, Cambridge, England, 2000).

[59] G. Agrawal, *Applications of Nonlnear Fiber Optics* (Academic Press, New York, 2001).

[60] R. K. Jain and R. C. Lind, J. Opt. Soc. Am. **73**, 647 (1983).

[61] P. Roussignol, D. Ricard, J. Lukasik, and C. Flytzanis, J. Opt. Soc. Am. B **4**, 5 (1987).

[62] J. Warnock and D. D. Awschalom, Phys. Rev. B **32**, 5529 (1985).

[63] A. E. Ekimov, A. L. Efros, and A. A. Onushchenko, Solid State Commun **56**, 921 (1985).

[64] L. E. Brus, J. Chem. Phys. **80**, 403 (1984).

[65] E. Hanamura, Solid State Commun **62**, 465 (1987).

[66] T. Takagahara, Phys. Rev. B **36**, 9293 (1987).

[67] K. M. Luung, Phys. Rev. A **33**, 2461 (1986).

[68] D. S. Chemla and D. A. B. Miller, Opt. Lett. **11**, 522 (1986).

[69] G. Jungk, Phys. Status Solid B **146**, 335 (1988).

[70] D. Stroud and P. M. Hui, Phys. Rev. B **37**, 8719 (1988).

[71] A. E. Neeves and M. H. Birnboim, J. Opt. Soc. Am. B **6**, 787 (1989).

[72] J. C. M. Garnett, Philos. Trans. T. Soc. London **203**, 385 (1904).

[73] J. C. M. Garnett, Philos. Trans. T. Soc. London **205**, 237 (1906).

[74] H. A. Lorentz, *Theory of Electrons*, 2nd ed. (Dover, New York, 1952).

[75] D. A. G.Bruggeman, Ann. Physik (Leipzig) **24**, 636 (1935).

[76] R. Landauer, J. Appl. Phys. **23**, 779 (1952).

[77] D. Bergman, Phys. Rep. **43**, 379 (1978).

[78] K. P. Yuen and K. W. Yu, J. Phys.: Condens. Matter **9**, 4669 (1997).

[79] W. J. Wen, H. R. Ma, W. Y. Tam, and P. Sheng, Phys. Rev. E **55**, R1294 (1997).

[80] Y. Gu and Q. H. Gong, Phys. Rev. B **67**, 014209 (2003).

[81] K. W. Yu and J. T. K. Wan, Computer Physics Communications **129**, 177 (2000).

[82] C. Atkinson and R. D. List, Int. J. Eng. Sci. **16**, 717 (1978).

[83] P. Gu and F. Erdogam, Int. J. Solids Struct. **38**, 1 (1997).

[84] Z. H. Jin and N. Noda, Int. J. Eng. Sci. **31**, 793 (1993).

[85] N. Noda and Z. H. Jin, Int. J. Solids Struct. **30**, 1039 (1993).

[86] X. Zhu, Q. Wang, and Z. Meng, J. Mater. Sci. Lett. **14**, 516 (1995).

[87] A. J. Sanchez-Herencia, R. Mereno, and J. R. Jurado, J. Eur. Ceram. Soc. **20**, 1611 (2000).

[88] G. Q. Gu and K. W. Yu, Acta Phys. Sin. **40**, 709 (1991).

[89] G. Fuhr and P. I. Luzmin, Biophys. J. **50**, 789 (1986).

[90] K. L. Chan, P. R. C. Gascoyne, F. F. Becher, and P. Pething, Biochim. Biophys. Acta **1349**, 182 (1997).

[91] Z. H. S. Shtrikman, J. Appl. Phys. **33**, 3125 (1962).

[92] J. P. Huang, K. W. Yu, G. Q. Gu, and M. Karttunen, Phys. Rev. E **67**, 051405 (2003).

[93] L. Dong, G. Q. Gu, and K. W. Yu, Phys. Rev. B **67**, 224205 (2003).

[94] G. Q. Gu and K. W. Yu, J. Appl. Phys. **94**, 3376 (2003).

[95] V. L. Sukhorukov, G. Meedt, M. Kürschner, and U. Zimmermann, J. Electrostatics **50**, 191 (2001).

[96] H. C. V. de Hulst, *Light Scattering by Samll Particles* (Dover, New York, 1981).

[97] R. Rojas, F. Claro, and R. Fuchs, Phys. Rev. B **37**, 6799 (1988).

[98] G. W. Milton, *The Theory of Composites* (Cambridge University Press, Cambridge, 2002).

[99] A. A. Lucas, L. Henrard, and P. Lambin, Phys. Rev. B **49**, 2888 (1994).

[100] H. Sun and K. W. Yu, Phys. Rev. E **67**, 011506 (2003).

[101] H. Grull *et al.*, Europhys. Lett. **50**, 107 (2000).

[102] S. G. Lu *et al.*, Appl. Phys. Lett. **82**, 2877 (2003).

[103] G. L. Fischer *et al.*, Phys. Rev. Lett. **74**, 1871 (1995).

[104] J. P. Huang and K. W. Yu, Appl. Phys. Lett. **85**, 94 (2004).

[105] K. P. Yuen, M. F. Law, K. W. Yu, and P. Sheng, Phys. Rev. E **56**, R1322 (1997).

[106] J. Bergman and D. Stroud, Solid State Physics **46**, 148 (1992).

[107] G. W. Milton, J. Appl. Phys **52**, 5286 (1980).

[108] R. C. McPhedran and G. W. Milton, Phys. A: Solids Surf. **26**, 207 (1981).

[109] J. P. Huang, L. Dong, and K. W. Yu, Europhys. Lett. **67**, 854 (2004).

[110] L. Gao, J. P. Huang, and K. W. Yu, Phys. Rev. E **67**, 021910 (2003).

[111] T. C. Choy, A. Alexopoulos, and M. F. Thorpe, Proc. R. Soc. London, Ser. A **454**, 1993 (1998).

[112] H. Morgan, M. P. Hughes, and N. G. Green, Biophys. J **77**, 516 (1999).

[113] C. Marquet, A. Buguin, L. Talini, and P. Silberzan, Phys. Rev. Lett. **88**, 168301 (2002).

[114] J. P. Huang, M. Karttunen, K. W. Yu, and L. dong, Phys. Rev. E **67**, 021403 (2003).

[115] J. P. Huang, K. W. Yu, and G. Q. Gu, Phys. Lett. A **300**, 385 (2002).

[116] J. P. Huang *et al.*, Phys. Rev. E **69**, 051402 (2004).

[117] J. P. Huang and K. W. Yu, J. Chem. Phys. **121**, 7526 (2004).

[118] G. Q. Gu, K. W. Yu, and P. M. Hui, J. Chem. Phys. **116**, 10989 (2002).

[119] J. P. Huang and K. W. Yu, Opt. Lett. **30**, 275 (2005).